The APPEA Journal 2018, **58**, 209–237
https://doi.org/10.1071/AJ17049

Peer reviewed paper

Helium in the Australian liquefied natural gas economy

Christopher J. Boreham[A,D], *Dianne S. Edwards*[A], *Robert J. Poreda*[B], *Thomas H. Darrah*[C], *Ron Zhu*[A], *Emmanuelle Grosjean*[A], *Philip Main*[A], *Kathryn Waltenberg*[A] *and Paul A. Henson*[A]

[A]Geoscience Australia, GPO Box 378, Canberra, ACT 2601, Australia.
[B]University of Rochester, Rochester, NY 14627, USA.
[C]Smart Gas Sciences, HCR 67, Box 3, Wilburton, PA 17888, USA.
[D]Corresponding author. Email: chris.boreham@ga.gov.au

Abstract. Australia is about to become the premier global exporter of liquefied natural gas (LNG), bringing increased opportunities for helium extraction. Processing of natural gas to LNG necessitates the exclusion and disposal of non-hydrocarbon components, principally carbon dioxide and nitrogen. Minor to trace hydrogen, helium and higher noble gases in the LNG feed-in gas become concentrated with nitrogen in the non-condensable LNG tail gas. Helium is commercially extracted worldwide from this LNG tail gas. Australia has one helium plant in Darwin where gas (containing 0.1% He) from the Bayu-Undan accumulation in the Bonaparte Basin is processed for LNG and the tail gas, enriched in helium (3%), is the feedstock for helium extraction. With current and proposed LNG facilities across Australia, it is timely to determine whether the development of other accumulations offers similar potential. Geoscience Australia has obtained helium contents in ~800 Australian natural gases covering all hydrocarbon-producing sedimentary basins. Additionally, the origin of helium has been investigated using the integration of helium, neon and argon isotopes, as well as the stable carbon ($^{13}C/^{12}C$) isotopes of carbon dioxide and hydrocarbon gases and isotopes ($^{15}N/^{14}N$) of nitrogen. With no apparent loss of helium and nitrogen throughout the LNG industrial process, together with the estimated remaining resources of gas accumulations, a helium volumetric seriatim results in the Greater Sunrise (Bonaparte Basin) > Ichthys (Browse Basin) > Goodwyn–North Rankin (Northern Carnarvon Basin) accumulations having considerably more untapped economic value in helium extraction than the commercial Bayu-Undan LNG development.

Keywords: Australia, argon, carbon dioxide, helium, LNG, neon, nitrogen, noble gas, remaining hydrocarbon resources, stable isotopes.

Received 15 December 2017, accepted 15 February 2018, published online 28 May 2018

Introduction

Australia has substantial gas resources, being the third-largest energy resource behind coal and uranium (Skirrow *et al*. 2013; AERA 2016). A significant proportion of these gas resources are exported as liquefied natural gas (LNG). These LNG projects are supplied by offshore gas accumulations in northern and western Australia and by onshore coal seam gas (CSG) in eastern Australia (APPEA 2017). The LNG is exported to northern markets; Japan, China, South Korea and Taiwan are the most significant established importers, and India is an emerging market (APPEA 2017). It is expected that in 2018, Australia will surpass Qatar as the world's largest LNG producer (AERA 2016). As a consequence of the LNG refining process that predominately condenses methane to a liquid, the other components in the original gas stream are either retained or discarded. For example, carbon dioxide (CO_2) is initially removed, natural gas liquids (C_{2+} hydrocarbons) are retained and the non-condensable components, predominantly nitrogen (N_2), are generally disposed of into the atmosphere. This component is referred to as the N_2-enriched tail (purge, end flash) gas (Reinoehl 2012). Consequently, minor components, including helium (He), are further concentrated within the tail gas. With the large volumes of gas passing through the LNG processing plant, commercial opportunities arise for further helium extraction utilising the tail gas, where the original helium concentration is as low as 0.04% (Daly 2005). Australia has one helium extraction facility, operated by BOC since 2010 at the Darwin Helium plant (Manufacturers' Monthly

2010), where their helium-feed gas is the tail gas from the ConocoPhillips LNG processing of the Bayu-Undan gas accumulation in the Bonaparte Basin (ConocoPhillips 2017).

This paper reviews the anthropogenic uses of helium, summarises the helium concentration in Australia's producing offshore and onshore gas accumulations and delineates geochemical and geological factors contributing to the origin and distribution of helium in Australian natural gases. Importantly, this study presents a ranking methodology for current and proposed LNG projects for their capacity to supply a helium-enriched tail gas that may be deemed suitable for further helium extraction. Future exploration opportunities delivered via acreage release will provide the first step in discovering more natural gas and helium resources in Australia (DIIS 2017).

Uses for helium

The noble gas helium is a critical commodity of strategic importance to high-technology fields with applications in defence, medicine, manufacturing, energy and scientific research (Cai *et al*. 2012; Hamak 2013). A reliable supply of helium into the future is necessary to ensure the continuation of these applications as well as enabling the emergence of new technologies in energy production, transport and information technology.

Soon after the discovery of the noble gas helium in natural gas at the turn of the 20th Century (Cady and McFarland 1907), the United States of America (USA) government realised the strategic value of helium. The first-ever helium plant was built by the US Army in 1915 in Petrolia, Texas, but helium was never sold commercially (Seibel and Kennedy 1934). Further helium plants at Fort Worth and Amarillo in Texas produced helium at around 10 million cubic feet (MMcf) per year. By 1935, the price of helium dropped from US$2.5 million (>$50 million present-day equivalent) to US$30 (US$540 present-day equivalent) per thousand cubic feet (Mcf) (American Chemical Society National Historic Chemical Landmarks 2000). The monopoly of helium sales by the US government was effectively broken in the 1990s when other countries came into the market, mainly because of the global increase in LNG production. Furthermore, drawdown of the US Bureau of Land Management (BLM) Cliffside helium reserve (National Materials Advisory Board 2010) helped create a gap in the helium market. These factors have enabled supply and demand to dictate helium pricing (Cai *et al*. 2012), and in today's market helium is over five times cheaper than in 1935.

Helium usage varies from year to year, and detailed data on global usage are limited (Nuttall *et al*. 2012*a*; and references therein). The US Geological Survey (USGS) collects yearly statistics on helium usage within the USA. Fig. 1*a* compares the usage of helium over the past decade and Fig. 1*b* shows that the USA and Qatar are the largest producers of helium worldwide.

Helium is chemically and physically unique, being the only gas that is not a solid below 14 K and it remains a liquid at 0 K (at atmospheric pressure) allowing its use as a coolant at extreme temperatures. This property is utilised in cryogenic applications, e.g. magnetic resonance imaging instruments and superconductors, which are entirely dependent on helium (Cai *et al*. 2012). Of note is CERN's Large Hadron Collider that individually requires a supply of 10–15 MMcf (283–425 Mm^3)

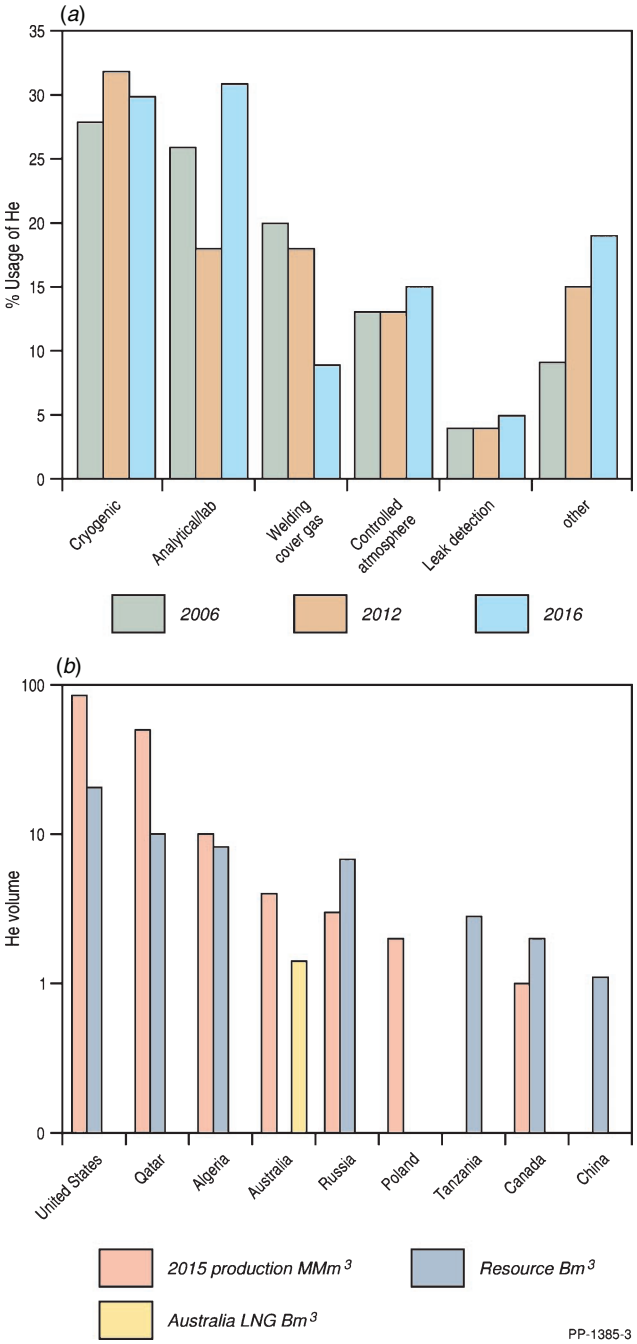

Fig. 1. Graphical representation of (*a*) the percent usage of He against type of use in the USA over the past decade for 2006 (USGS 2007), 2012 (USGS 2012) and estimate for 2016 (USGS 2017*b*), and (*b*) the volume of He commodity available in each country: 2015 He production (million cubic metres (MMm^3)) (USGS 2017*b*), He resource estimate (billion cubic metres (Bm^3)) (USGS 2017*b*) and Australian He resource (Bm^3) from liquefied natural gas (LNG) (1.67 Bm^3; sum total of remaining helium resource in Table 3).

of helium per year for cryogenic purposes (Claudet *et al*. 2015; CERN 2017).

Helium acting as an inert atmosphere is used in many types of high-tech fabrication, including the manufacture of fibre-optic cables, computer chips and semiconductors. In the fibre-optics industry, helium is required to quickly cool the fibre as it is drawn from a furnace and to prevent bubbling in the fibre (Cai *et al*. 2012). The electronics industry is a significant user of helium for manufacturing of liquid crystal displays and plasma televisions (National Materials Advisory Board 2010). Helium also has many scientific and laboratory uses, such as being used in ultra-high purity as a carrier gas in chromatography (including use at Geoscience Australia (GA)) and in low temperature physics experiments.

Historically, the low helium price in the USA has led to its widespread use as a welding cover gas (National Materials Advisory Board 2010), remaining inert due to its highest ionisation potential compared with any other element or compound. However, the decline in helium in welding in 2016 (Fig. 1*a*) is in contrast to the increased domestic consumption of helium that same year (USGS 2017*a*, 2017*b*). The recent sharp decrease in its use as a welding gas is perhaps in response to an overall steady decline in helium production (USGS 2012) and a transition to other unreactive gases (e.g. argon).

Helium is used in leak detection because it is the smallest molecule and will pass through very small defects in a system. The abundance of helium in the atmosphere is very low, so even a small leak can be easily detected. Leak detection is also pertinent to the electronics and advanced materials industries, scientific research and the space industry (National Materials Advisory Board 2010). Other applications of helium are many and varied:

- Helium is lighter than air; therefore, it has uses for lifting, for example, party and parade balloons, weather monitoring, defence (surveillance and reconnaissance) and scientific research balloons and blimps (National Materials Advisory Board 2010);
- In rocketry, helium is used to flush hydrogen (H_2) pressurised fuel tanks (e.g. a USA space shuttle launch used ~1 MMcf (28.3 Mm^3) of helium (NASA 2001));
- Other medical uses of helium include lung tissue visualisation, heart catheterisation, laser treatment and asthma treatment (Bureau of Land Management 2017);
- Very high sonic velocity in helium has been exploited in sprayed metal coatings (Cai *et al*. 2012);
- Helium's low susceptibility to becoming radioactive and its relatively high thermal conductivity means that it is used for heat transfer in some gas-cooled nuclear reactors (Cai *et al*. 2012);
- Satellites employ helium to cool telescopes for improved image resolution;
- Helium is mixed with either oxygen or oxygen and nitrogen to extend diving depths (Smith *et al*. 2004);
- The stable ^{3}He isotope—man-made from tritium (^{3}H) decay and up to 100 million times rarer than the ^{4}He isotope in the natural environment—is increasingly used in neutron detectors for heightening security measures (Cartwright 2012);
- The stable ^{3}He isotope is being investigated for its use for nuclear fusion power that produces non-radioactive waste (Smith *et al*. 2004); however, this application is limited by the isotope's scarcity compared with ^{4}He;
- The stable ^{3}He isotope is being used in lung cancer screening and imaging; and
- Helium is being used in surface prospecting where high helium anomalies may indicate sub-surface petroleum accumulations (Riley 1980).

In the future, helium will remain a critical commodity for a wide range of low-carbon technologies and guaranteed supply will depend on an increased focus of recycling (Smith *et al*. 2004) and governments and industries working together both locally (Riley 1980) and across the globe (Smith *et al*. 2004; Nuttall *et al*. 2012*b*; Scurlock and Francis 2012).

Global helium production and resources

In 2015, global helium production was 5.51 billion cubic feet (Bcf) (156 million cubic metres (MMm^3)), coming predominantly from the USA and Qatar (Table 1), with Australia contributing a very minor 0.14 Bcf (4 MMm^3) from BOC's Darwin helium processing plant (USGS 2017*b*). The USGS (2017*b*) estimated that the 2015 global helium market for Grade-A (≥99.997%) helium was worth around US$1.1 billion.

As stated by the USGS (2017*a*), the best available global helium resource estimates, as of 31 December 2006, are 1.87 trillion cubic feet (Tcf) (51.9 billion cubic metres (Bm^3)); a USGS update is currently underway and will take several more years to complete. Fig. 1*b* is a summary of these 2006 global helium resource estimates with commercial recovery possible from helium contents as low as 0.04% (see also Table 1) because of the processing of gas for LNG, and in some instances, domestic gas. At the other extreme, a large new potential helium resource in Tanzania has been discovered where the gas has a helium content up to 10.2% (Helium One 2017*a*) (Fig. 1*b* and Table 1).

The USA is the largest user and has the largest reserves of helium worldwide (Fig. 1*b*) with Qatar suppling around $^1/_3$ of global helium in 2016 (USGS 2017*b*). The domestic supply of the USA will continue to be dominated by the BLM's annual auction from the federal helium storage at Cliffside Field near Amarillo until cessation on or before end-September 2021 (USGS 2017*a*). This depleting helium reserve, together with the transient limited helium output from Qatar in 2017 through political sanctions, has led to a forecast of a global helium deficit commencing in 2020 (Helium One 2017*b*). Of note is that Hooker (2012) predicted an accelerating helium shortfall after 2016. However, these transient shortfalls are to be expected with helium predicted to be available via the petroleum industry from natural gas for at least another 50 years before ending early next century (Nuttall *et al*. 2012*a*, 2012*b*).

In response to the perceived near-future volatility in the helium supply chain and to help foster an expansion in local helium production, GA has undertaken an assessment of Australia's LNG feedstocks to determine the crude helium by-product's potential for future growth in industrial helium production.

Table 1. Location of global helium extraction plants

N/A = information not available, BLM = Bureau of Land Management, — = not applicable

Country	2015 production MMm^3 (MMcf)[A]	% of global production	Plant	Field	Reservoir rocks	Reserves (Mm^3)[A]	Resources Bm^3 (Bcf)[A]
USA	88 (3108)[B]	56	BLM enrichment unit Doe Canyon, Colorado Ladder Creek, Colorado Harley Dome, Utah Shute Creek, Wyoming Big Piney, Wyoming Plants on BLM pipeline, Kansas, Oklahoma, Texas	Cliffside (1.9% He)[1,C] Doe Canyon (0.35% He)[2] Various[3] Harley Dome (7% He)[4] LaBarge (0.7% He)[5,E] LaBarge (0.7% He)[5,E] Hugoton-Panhandle (0.5% He)[6]	Permian Bush Dome brown dolomite[1] Mississippian Leadville Limestone[2] N/A Jurassic Entrada Sandstone[4] Mississippian Madison Limestone[5] Mississippian Madison Limestone[5] Permian carbonates[7]	3900	20.6 (727)
Qatar	49 (1730)	31	Ras Laffan	North Field (0.04% He)[8,F]	Permo-Triassic limestones[9]		10.1 (357)
Algeria	10 (353)	6	Helios, Arzew Helison, Skikda	Hassi R'Mel (0.19% He)[10] Hassi R'Mel (0.19% He)[10]	Triassic sandstones[11] Triassic sandstones[11]	1800	8.2 (290)
Australia	4 (141)	3	Darwin, Northern Territory	Bayu-Undan (0.1% He)[D]	Jurassic Plover Formation[D]		1.8 (64)[D]
Russia	3 (106)	2	Orenburg	Orenburg (up to 0.06% He)[12]	Carboniferous-Permian carbonates[13]	1700	6.8 (240)
Poland	2 (71)	1	Odolanow	Polish Lowland (0.4% He)[14]	Permian Rotliegend, Zechstein Limestone and Main Dolomite formations[15]	25	
Canada	1 (35)	1	Weil Canadian Helium Inc.	Mankota (up to 1.4%)[16] Wilhelm (up to 2% He)[16]	Cambrian Deadwood Formation[16] Cambrian Deadwood Formation[16]		2 (71)
China			N/A	Weiyuan (up to 0.34%)[17]	Sinian and Pre-Sinian strata[17]		1.1 (39)
Tanzania			_	Ruksa (2.5–4.2%He)[18] Rukwa (8–10.2%He)[19]	N/A		2.8 (99)[19]
World Total (rounded)							156 (5509)

[A]data from USGS (2017*b*) for global helium reserves and resources unless otherwise noted.
[B]Extracted from natural gas + Cliffside Field Government Reserve.
[C]Average before injection began in 1963; subsequent gas injected in the Bush Dome reservoir raised helium to 29.4%[20].
[D]This study.
[E]He content of 19% for the tail gas feeding the plant (Linde 2017).
[F]He content of 32% for the tail gas feeding the plant (Linde 2017).
[1]Tade (1967); [2]Shelton *et al*. (2016); [3]Hubler (2004); [4]Ward and Pierce (1973); [5]Merrill *et al*. (2014); [6]Jordan (2016); [7]Ballentine and Sherwood-Lollar (2002);
[8]Rufford *et al*. (2014); [9]Aali *et al*. (2006); [10]Reinoehl (2012); [11]Boote *et al*. (1998); [12]Hooker (2012); [13]Peterson and Clarke (1983); [14]Jones and Stacey (1974); [15]Markiewicz and Winnicki (2013);
[16]Yurkowski (2016); [17]Ni *et al*. (2014); [18]Hand (2016); [19]Helium One (2017*b*); [20]Peterson (2012).

Origin of helium

Abundance and isotopic composition

Helium makes up around ¼ of the mass of the Universe (Nath 2013). The atmospheric reservoir of helium is in dynamic equilibrium with continual loss of helium into space (calculated residence time of 1 Ma for ^{3}He in the atmosphere; Allègre *et al*. 1987) and replenishment mainly through volcanic activity, which is supplemented by the decay of tritium, resulting in a present-day concentration of 5.24 parts per million (ppm) vol/vol) (de Laeter *et al*. 2003; Sano *et al*. 2013). Of the other noble gases, neon (Ne) is partially lost to space (Sarda *et al*. 1988), while atmospheric argon (Ar) and the heavier noble gases, krypton (Kr) and xenon (Xe), have remained within the atmosphere for billions of years (Allègre *et al*. 1987). The noble gas isotopic ratios have remained constant from at least the Phanerozoic (Allègre *et al*. 1987).

Helium was first discovered on Earth in 1895 (for helium's controversial history in the late 19th century see Jensen 2004 and Nath 2013) as the inert gas released after acid digestion of the uranium-bearing, radioactive mineral clèveite (Ramsay 1895), in quick succession in groundwater (Crookes 1897, 1898) and in the terrestrial atmosphere (Baly 1898; Crookes 1898). A decade later, helium was found to be almost ubiquitous in natural gas (Cady and McFarland. 1907), and in 1939 the existence of two stable isotopes of helium (^{3}He and ^{4}He) was established (Alvarez and Cornog 1939). For over a century, natural gas has continued to be the sole source for helium extraction, principally from wells within the USA with >0.3% helium (Gage and Driskill 2004; and references therein). Helium extraction from air, with its enormous reservoir of 811 Tcf or 23 trillion cubic metres (Tm^3), could be a niche industry when associated with neon extraction from air processing (Clarke *et al*. 2012). However, in the future, larger volumes of air-extracted helium will need to be cost competitive with other sources, such as natural gas extraction (Clarke and Clare 2012).

The enormous volumes of gas processed by the global LNG production industry have enabled more countries to extract helium from the tail gas. Current global helium producing plants outside of the USA are using initial helium molar percentages between 0.04% and 2% (Table 1); with the low helium concentrations (down to 0.04–0.06‰) in natural gas successfully commercialised in Qatar (Daly 2005) and Russia (Hooker 2012). Therefore, the future potential for helium production is linked with the rising demand for LNG and the location (e.g. onshore or offshore) and capacity of the associated LNG processing plants. In addition, natural gas for Australian domestic use may provide future helium extraction potential.

Helium concentrations in global natural gases show a wide range from <0.005% up to around 10%. For example, reservoirs in the Permian Basin in western Texas and south-eastern New Mexico, USA, have 9.74% helium (Tongish 1980), and the Rukwa Project, Tanzania, has 10.2% helium (Helium One 2017*a*). In the Amadeus Basin in Australia, gas in Mt Kitty-1 has 9.0% helium (McInnes *et al*. 2017).

Various classification schemes for helium abundance appear in the literature:

- trace helium contents are up to 0.005% (Tongish 1980),
- very low helium <0.05% (Gage and Driskill 2004),
- low helium <0.1% (Xu *et al*. 1991),
- helium-rich >0.1% (Ballentine and Sherwood Lollar 2002),
- helium wells >0.3% (Gage and Driskill 2004),
- economic helium wells >0.5% (Zartman *et al*. 1961), and
- high helium content is >1% (Xu *et al*. 1991).

Herein 'high helium' is regarded as being >0.5%. In the context of LNG and associated helium purification, natural gases down to 0.04% helium are proven to be commercial, although the original abundance of nitrogen (N_2), as the dominant non-condensable gas, in the natural gas must also be considered.

To best understand the origin, occurrence and distribution of helium in natural gas, it is important to identify genetic and/or non-associated links with the other noble gases, as well as with the organic and inorganic gases. The conservative nature of helium and nitrogen will govern the enrichment factor (N_2/He being considered constant; also see section 'Helium from LNG processing') from the raw gas stream to the LNG N_2 dominated- and He-enriched tail gas. Ballentine and Sherwood Lollar (2002) reported that gases with helium concentrations >0.1% contain high nitrogen with few exceptions and that the N_2/He ratios vary between ~5 and 50. In the Australian Bayu-Undan gas accumulation/Darwin LNG/Darwin Helium supply chain the N_2/He ratio varies from 19 to 42 (3.4–3.9% N_2, 0.09–0.21% He) for the Bayu-Undan gases from individual wells, and in the Darwin LNG tail gas/BOC Darwin helium-feed gas the N_2/He ratio is 31 with 3% helium (Linde 2010). Note that Clarke *et al*. (2012) list an incorrect Darwin LNG feed-in and tail gas of 0.015% He and 50% He, respectively.

Sub-surface sources of helium

In the subsurface, the three sources of helium in natural gases are from the mantle, crust and groundwater (Byrne *et al*. 2017; and references therein); the latter is initially derived from the dissolution of atmospheric gases either at the time of sedimentation or much later through exchange with formation water. All sources are dominated by ^{4}He but the relative abundance of ^{3}He can help infer source inputs. The ratio of ^{3}He to ^{4}He is defined as R. The present-day atmospheric ^{3}He/^{4}He ratio = 1.39×10^{-6} is also denoted as Ra (R/Ra = 1). Compared with the atmospheric ^{3}He/^{4}He ratio, Mid-Ocean Ridge Basalt (MORB)-derived helium has an average R/Ra = 8, the helium (as dissolved air) in groundwater has an R/Ra = 0.985 and crustal-derived helium displays an average of R/Ra = 0.02 (Ballentine *et al*. 1991). The elemental composition of uranium (^{235}U and ^{238}U), thorium (^{232}Th) (both are the radiogenic parents of ^{4}He) and lithium (^{6}Li) (the nucleogenic parent of ^{3}He) in the rock forming minerals will ultimately determine the 'average' R/Ra. However, R/Ra ratios can vary considerably within subsurface reservoirs, with R/Ra ratios in the crust varying from <0.01 to 0.05 (Ni *et al*. 2014; Darrah *et al*. 2015; Moore *et al*. 2017; and references therein), upper mantle ~2 to 8 R/Ra (Darrah *et al*. 2015) and lower mantle up to 40 R/Ra (Poreda *et al*. 1986). Evolutionary mantle models predict an initial R/Ra ratio >100 (Tolstikhin and Marty 1998),

while a R/Ra ratio of 230 is assumed for the initial 'un-degassed' (i.e. primitive, never melted) Earth's mantle, which is between the inferred R/Ra ratio of 120 and 330 for the initial solar nebula and the solar wind, respectively (Class and Goldstein 2005; and references therein). The much higher ^{3}He content within the mantle reflects the inherited primordial ^{3}He from when the Earth was formed, with the upper mantle being almost completely degassed compared with the lower mantle (Allègre *et al*. 1987; Tolstikhin and Marty 1998). Alternatively, mantle convection and magmatism results in variable helium isotopic depletion where prolonged isolation of plume sources preserves the high ^{3}He/^{4}He ratio (i.e. in ocean island basalts (OIB)) compared with a more degassed mantle during prolonged continent and oceanic crust formation (i.e. MORB) wherein radiogenic ^{4}He makes a higher contribution over time to mantle helium (Class and Goldstein 2005).

The crustal noble gas isotopes are produced at known rates and in known relative proportions, and therefore, quantitative analysis and age determination is possible (Ballentine and Sherwood Lollar 2002; and references therein). The higher radiogenic production rates of ^{4}He in crustal versus mantle sources is intimately linked with the higher U and Th contents in the former compared with the latter (Ballentine and Burnard 2002; Class and Goldstein 2005), with the lowest radioactive metal contents associated with the highest ^{3}He/^{4}He ratios (e.g. OIB) (Class and Goldstein 2005). However, mixed sources are difficult to deconvolute based on helium isotope systematics alone and commonly require the combinations of heavier noble gas abundance and isotopic compositions to differentiate the three end-member inputs (Ballentine *et al*. 1991). For example, ^{20}Ne and ^{36}Ar are considered entirely atmospheric-derived, so departures in isotopic ratios in natural gases compared with atmospheric ratios (^{4}He/^{20}Ne in air = 0.32 (Ballentine and Sherwood Lollar 2002) and ^{20}Ne/^{36}Ar in air = 0.55 (Ballentine *et al*. 1991)), give clues to additional source inputs (Gilfillan *et al*. 2009; Hunt *et al*. 2012; Darrah *et al*. 2014, 2015). The water solubility of helium and neon are similar; however, solubility differences amongst the heavier noble gases add an extra complication, with the ^{20}Ne/^{36}Ar ratio in air-saturated water (ASW) being lower than atmospheric by five times (Ballentine *et al*. 1991). Intra-element ratios are also employed with ^{40}Ar/^{36}Ar values greater than air (i.e. >295.5; Zartman *et al*. 1961; Hunt *et al*. 2012) being attributed to the addition of potassium (K)-derived radiogenic ^{40}Ar (denoted as ^{40}Ar*; Ballentine *et al*. 1991), which could potentially change through time. Ballentine and Sherwood Lollar (2002) also noted that the mantle-derived ^{40}Ar/^{36}Ar ratio is extremely high (28 000). In the noble gas analysis of vertically stacked natural gas reservoirs in the Pannonian Basin, Hungary, Ballentine *et al*. (1991) used a combination of the above ratios to conclude that helium had a dominantly crustal source ($0.18 < R/Ra < 0.46$) and there is a depth increase in radiogenic ^{40}Ar* relative to atmospheric ^{20}Ne and ^{36}Ar. Furthermore, volumetric constraints required an additional input of an even deeper source of radiogenic ^{4}He. In the analysis of the Hugoton-Panhandle giant gas field, Ballentine and Sherwood Lollar (2002) concluded that the helium contribution to the reservoired gas was derived from a crustal source (R/Ra 0.14–0.25) and had a negligible atmospheric helium input based on the extremely high ^{4}He/^{20}Ne (>18 000) and ^{40}Ar/^{36}Ar (816–1156) ratios. Preferential release of ^{4}He over ^{40}Ar* from deep mineral grains below temperatures of ~200°C was also considered (Hunt *et al*. 2012; Darrah *et al*. 2014, 2015). There are numerous other literature examples of detailed analysis of noble gas isotope systematics applied to natural gases (see reviews by Hunt *et al*. 2012; Prinzhofer 2013; and Byrne *et al*. 2017). However, such a well- or field-specific analysis is outside the scope of this paper. Instead, we present a preliminary, basin-wide analysis of these geochemical datasets for Australian natural gases.

Geological controls on helium occurrence

Helium in natural gas accumulations gives a wide range in R/Ra ratios depending on the natural gas genesis, abundance of radioactive elements, outgassing efficiencies, accessibility to deep hot fluids, timing of magmatic input and time within the reservoir (Polyak and Tolstikhin 1985). Helium is readily released from minerals and transferred to underground fluids (magmatic/hydrothermal/pore water) where the helium isotopic composition is naturally averaged and can take on regional characteristics (Hunt *et al*. 2012; Darrah *et al*. 2014, 2015; Moore *et al*. 2017). During a magmatic event, injection of hot silicate-rich fluids carrying dissolved excess ^{3}He from the deep crust results in elevated R/Ra ratios that are primarily associated with the magmatic event, although the timing of the injection of molten fluid is not necessarily the age of the tectonic movement (Polyak and Tolstikhin 1985). After the magmatic activity has ceased, the R/Ra ratio declines to a background level within ~500 Ma due to the radiogenic input of ^{4}He (Polyak and Tolstikhin 1985). Oceanic rifts tend to have fluids with rather constant, but elevated, R/Ra ratios (7−9 Ra) indicative of MORB-like dominant mantle inputs, while continental rifting zones show the widest range in R/Ra (2−30 Ra), with the highest R/Ra ratios being associated with either plume heads or the most recent volcanic activity (Poreda *et al*. 1986, 1992; Darrah *et al*. 2013). Such is the case in the Otway Basin, where CO_2-rich natural gases have the highest mantle helium input (Watson *et al*. 2004). Areas above mantle plumes (hot spots) have consistently high R/Ra ratios (up to ~40 Ra), with values depending on whether the rising hot fluids tap into either the upper or lower mantle and/or mixes with recycled crustal components (Polyak and Tolstikhin 1985).

From an analysis of a large USGS database of natural gases, Brown (2010) has gleaned several geological principles and provided exploration guidelines for high helium (>0.5%) gases. Brown (2010) noted that the high helium gases generally occur either in shallow reservoirs at around 500 m, independent of reservoir age, or in older Paleozoic reservoirs at much greater depths. Furthermore, high helium gases show no correlation with the regional distribution of igneous bodies or (devolatilised) basement provinces, although basement faults and fractures could localise the vertical migration of helium-containing fluids (Brown 2010; and references therein). Helium dissolved in pore water and contact-transfer into an existing gas phase was the main gas exchange mechanism (Sathaye *et al*. 2016). Thus, higher helium-concentrated pore waters would eventuate where the sediment source had high uranium and/or thorium

contents, pore water volume is reduced by lower porosities and initial contact between sediment source-pore water would transfer the most helium. Therefore, exploration areas where high helium contents could accumulate following either fluid migration or the extensive removal of the dominant carrier phase (i.e. hydrocarbon oxidation, CO_2 dissolution) are favoured in reservoirs at shallow depth, with low temperatures and high salinity because helium is least soluble in this aqueous phase (Darrah *et al*. 2014, 2015; Harkness *et al*. 2017; Moore *et al*. 2017). Maximum exposure to pore water, as encountered in long distance migration, also assists in the concentration of helium. Exploration is also more favourable at the edges and migration fronts of supercharged petroleum systems and where the source rocks are marginally mature for gas generation, thereby reducing the dilution of helium with gaseous hydrocarbons, and in the case of intrusives, away from CO_2 occurrences. Since helium is the smallest molecule, a highly competent seal, particularly evaporites (salt (halite) or anhydrite) or unfractured shales, is a prerequisite (e.g. Cliffside field helium storage site (Peterson 2012) and the Amadeus Basin (Clarke *et al*. 2014; Boreham *et al*. 2018)).

Samples and methods

Helium has been detected in ~800 natural gases analysed by gas chromatography (GC) at GA, together with concentrations (in molar percent (%)) of H_2, N_2, CO_2, C_1-C_5 and C_{6+} hydrocarbons (Boreham and Edwards 2008). Many samples have complementary stable carbon ($^{13}C/^{12}C$) isotopic data for the individual C_1–C_5 gaseous hydrocarbons and CO_2, and stable nitrogen isotopes ($^{15}N/^{14}N$), obtained using the methods described in Boreham and Edwards (2008) and Chen and Boreham (2010), respectively. A subset of 252 natural gases from 216 wells was further analysed in the USA for noble gas isotopes by mass spectrometry (MS) at the University of Rochester, Smart Gas Sciences and The Ohio State University using methods outlined in Darrah *et al*. (2014, 2015).

Results and discussion

The wells with natural gases analysed for noble gas isotopes are shown in Fig. 2. Gases for all Australian sedimentary basins with either significant gas production and/or resources have been included in this study, with a main concentration of natural gas samples from offshore Western Australia. The reservoir ages range from the Paleo−Mesoproterozoic (McArthur Basin) to Cenozoic (Bass Basin). The Amadeus Basin contains gases with the widest reservoir age range spanning from the Neoproterozoic to Ordovician.

Geochemical characteristics of the hydrocarbon gases

The molecular and carbon isotopic composition of the gaseous hydrocarbons analysed for noble gas isotopes are summarised in Figs 3 and 4, which highlight the maturity and some aspects related to the source of the gas. The plot of the natural logarithms of methane/ethane (C_1/C_2) ratio versus the ethane/propane (C_2/C_3) ratio (Fig. 3) reveals that the Australian natural gases are generated over a wide maturity range but are mainly associated with primary gas generation from the organic matter (kerogen) within the source rock with fewer examples of secondary gas generation associated with additional higher maturity oil-to-gas cracking, as previously reported in Boreham *et al*. (2001). Gases that are biodegraded generally show elevated C_1/C_2 ratios from the input of biogenic methane and elevated C_2/C_3 ratios from the selective biodegradation of propane (Boreham *et al*. 2001; Harkness *et al*. 2017). Integration of the molecular composition (C_2/C_3) with the carbon isotopic difference between C_2 and C_3 (Fig. 4) corroborates the maturity and source interpretations based on the molecular compositions alone. Since there is a preference for ^{12}C to be consumed in the microbial degradation of gas, this results in a ^{13}C enrichment of the residual gas component (Boreham *et al*. 2001; Milkov 2011).

Helium contents and isotopic compositions

The frequency plot of the helium concentration (as determined by GC) in the Australian natural gases is shown in Fig. 5. Although basinal average He% is probably not a good measure of the helium distribution ('standard deviation' having a similar value to 'average'; for example see Table 3) it does provide a means for inter-basin comparison with average helium (data from GC analysis only and excluding gases with helium > 1% (Magee-1, 6.27% He (Pacific Oil and Gas 1992) and Mt Kitty-1, 9% He (McInnes *et al*. 2017)) ranging from 0.009% to 0.255% in the order Clarence-Moreton (0.009%) < Gippsland (0.014%) < Northern Carnarvon (0.023%) < Bass (0.025%) < Cooper (0.034%) < Bowen (0.041%) < Browse (0.049%) < Otway (0.051%) < Bonaparte (0.075%) < McArthur (0.119%) < Surat (0.126%) < Perth (0.154%) < Adavale (0.167%) < Amadeus (0.183%) < Canning (0.252%) < Gunnedah (0.255%) basins. The older reservoir and sedimentary rocks have more time for radiogenic ^4He production, and hence, generally show higher average helium content (Boreham *et al*. 2017). Helium concentrations between 0.005–0.099% show the highest frequency with an exponential decline in the number of natural gases with increasing helium concentrations up to around 10%. A similar trend is seen in the natural gases from the USA (Tongish 1980) but the proportion of gases with helium >0.1% is much greater in the USA. Although differences in the helium distributions between the natural gases from Australia and the USA are likely to be due, in a large part, to the local geological setting and history, a gas sampling bias towards USA gases having elevated helium contents cannot be ruled out (Brown 2010).

An initial deduction regarding the sources of helium can be obtained from the two stable helium isotopes, ^3He and ^4He. The log plot of ^4He versus ^3He concentrations includes the gradient lines following the trend for the commonly accepted values for mantle, air and crustal (radiogenic) helium sources (Fig. 6). Most Australian gases display helium isotope values consistent with a crustal origin. Notably, subsets of samples from the Bass, Bowen, Browse, Gippsland, Otway and Perth basins, among others, display intermediate values of R/Ra. From the log plot of ^4He concentration against the R/Ra ratio (Fig. 7), it is clear that the gases can be assigned to varying proportions of crustal, mantle and ASW. Gases with an exclusive crustal source

(*a*)

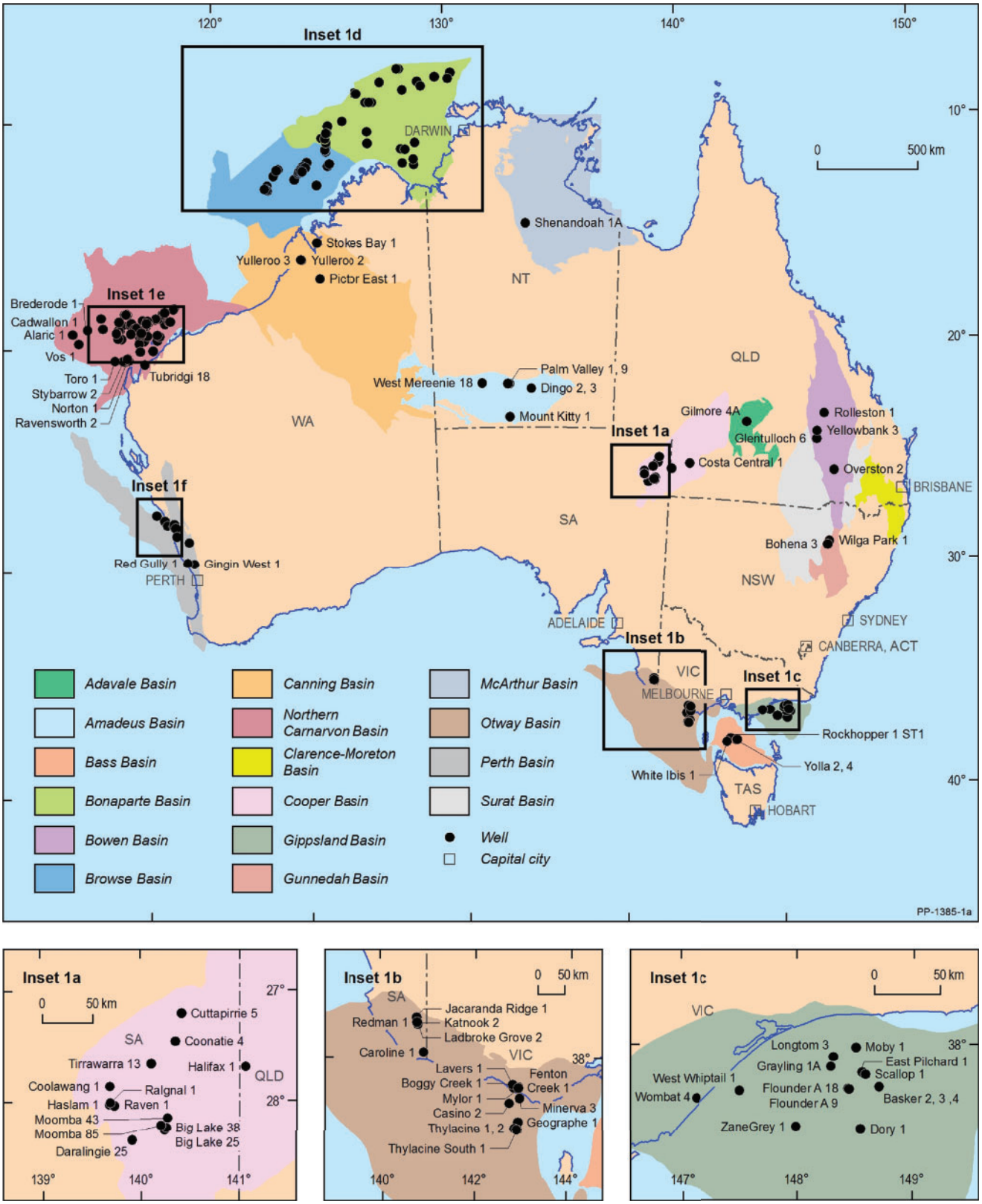

Fig. 2. (*a*) Location map of well test samples with noble gas data, including enlarged insets 1a, 1b and 1c. (*b*) Enlarged insets 1d, 1e and 1f.

(*b*)

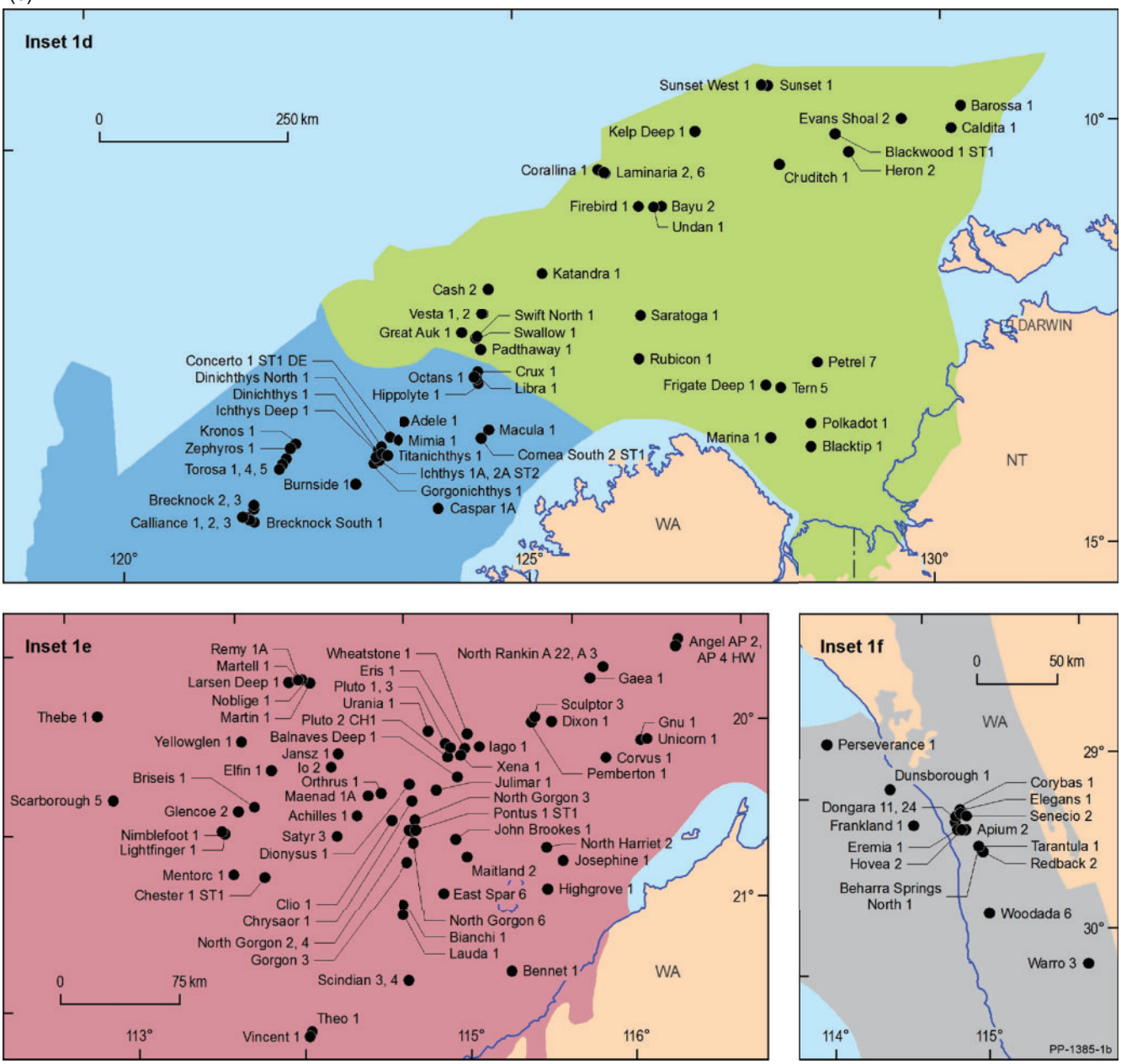

Fig. 2. (*continued*)

(R/Ra < 0.05) are from the Amadeus, Canning, Cooper, McArthur, Northern Carnarvon and Perth basins. Gases with R/Ra > 0.05 are considered to have a mixed helium source, including examples from the Adavale, Bass, Bonaparte, Bowen, Browse, Gippsland, Gunnedah, Otway and Perth basins. In addition to a crustal source, the contributions of mantle and/or air (where R/Ra < 1) can't be completely resolved using helium isotopes alone and additional isotopic data from higher noble gases is required (see section on 'Neon and Argon'). Significant Cenozoic volcanism in eastern Australia has resulted in a major mantle source (R/Ra > 1) occurring in some natural gases from the Bass, Gunnedah and Otway basins.

It is informative to delve a little deeper into the origin of helium to highlight the limitations in using only helium isotopes without attention to the other geological and geochemical datasets (also see next section 'Relationships between helium and other inorganic gases'). For example, surface heat flow is a combination of mantle and crustal inputs, and the general dipartite division of high heat flow between radiogenic heat flow in eastern Australia and sub-lithospheric (mantle) heat flow in western Australia (Hasterok and Gard 2016) may suggest concentration of ^{4}He in the former and ^{3}He in the latter regions. Obviously local radiogenic ^{4}He production over time will attenuate the ^{3}He content with lowering of R/Ra in the

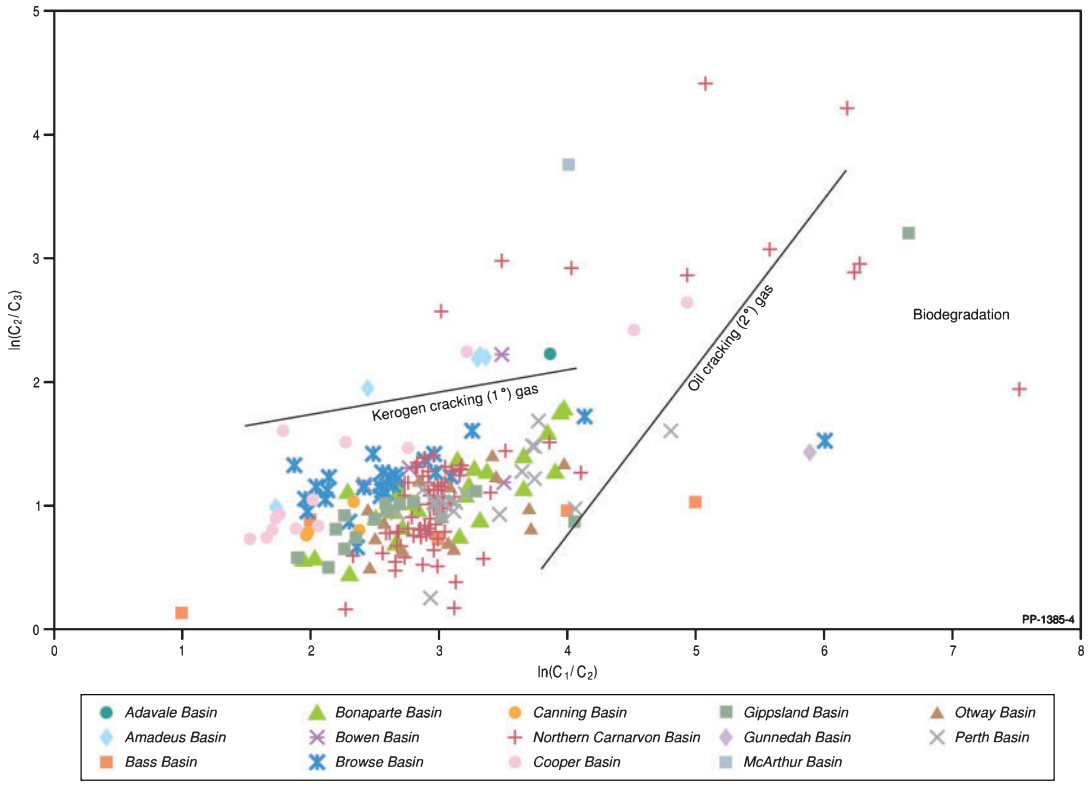

Fig. 3. Plot of ln methane%/ethane% versus ln ethane%/propane%. Modified after Tao *et al.* (2014).

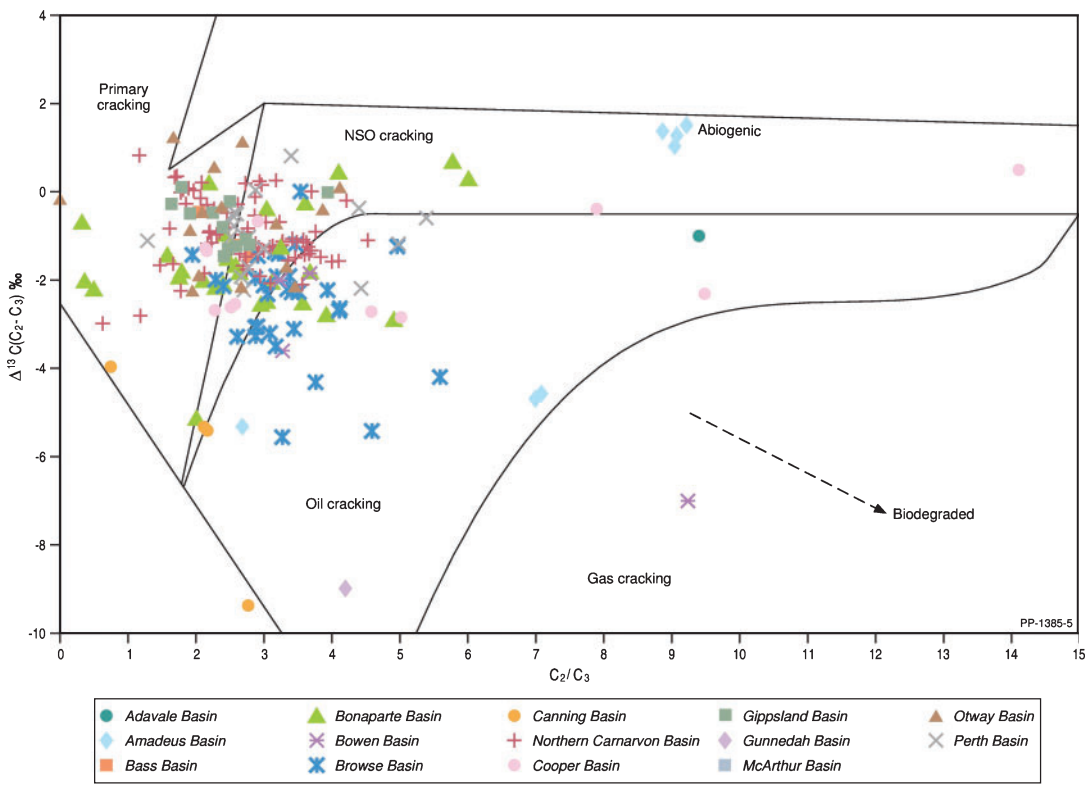

Fig. 4. Plot of ethane%/propane% versus carbon isotopic difference ($\Delta^{13}C$) between ethane and propane (‰). Note: McArthur Basin is off-scale with $C_2/C_3 = 42.6$ and $\Delta^{13}CC_2–C_3 = 1.78$‰, as are the biodegraded gases (most plotted in Fig. 3) having $C_2/C_3 > 15$ and $\Delta^{13}CC_2–C_3 < –10$‰. Modified after Lorant *et al.* (1998).

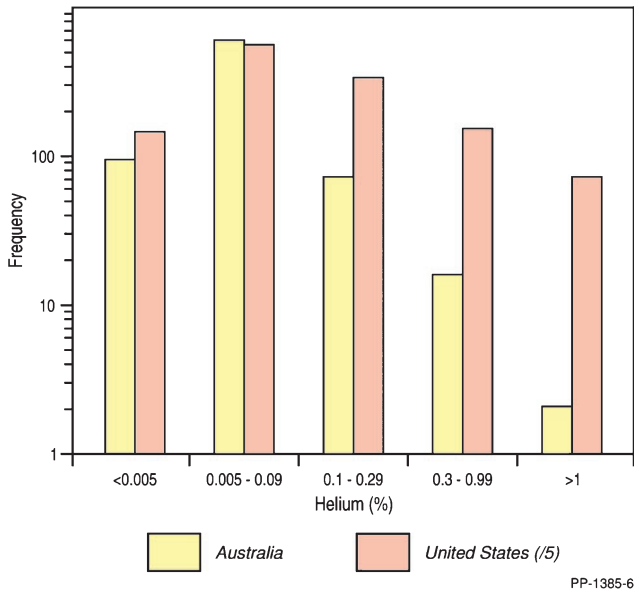

Fig. 5. Frequency plot of helium% (measured by gas chromatography (GC)) for Australian natural gases and natural gas wells from the USA (Tongish 1980). The number of USA wells is 6455 and the plot displays frequency divided by five in order to get similar displayed maximum values of frequency.

natural gas (e.g. Amadeus and McArthur basins; Figs 6 and 7). In addition, in central Australia the crustal contribution to heat flow is about twice that expected of the global-average continental crust (McLaren *et al*. 2003). This is a direct result of a higher than average concentrations of crustal radiogenic elements U and Th (McLaren *et al*. 2003), leading to ^{4}He. More restricted areas with high surface heat flow are outboard of the Browse and Perth basins (Cull and Conley 1983); interestingly, the first-order heat flow is relatively low and fairly constant throughout the North West Shelf (Cull and Conley 1983). The relative higher R/Ra in the Browse Basin (Fig. 7) may indicate a local area of higher sub-lithospheric heat flow (Hasterok and Gard 2016). Gases from the Canning Basin have the second highest average helium content with a dominant crustal helium source (Figs 6 and 7) and are in accord with a restricted hot spot in radiogenic heat flow in this region (Hasterok and Gard 2016). A high sub-lithospheric heat flow is also predicted along the eastern–south-eastern edge of Australia in response to much younger Cenozoic tectonism (Cull and Conley 1983; Hasterok and Gard 2016) and concur with natural gases with the highest mantle ^{3}He inputs (R/Ra > 1; Bass, Gunnedah and Otway basins; Fig. 7). A more detailed analysis between the evolution of helium content and R/Ra values in natural gases and heat flow is outside the scope of this paper. Another example is in the Browse Basin where the age of the oil/gas reservoirs creates complexity in discerning the origins of helium in the

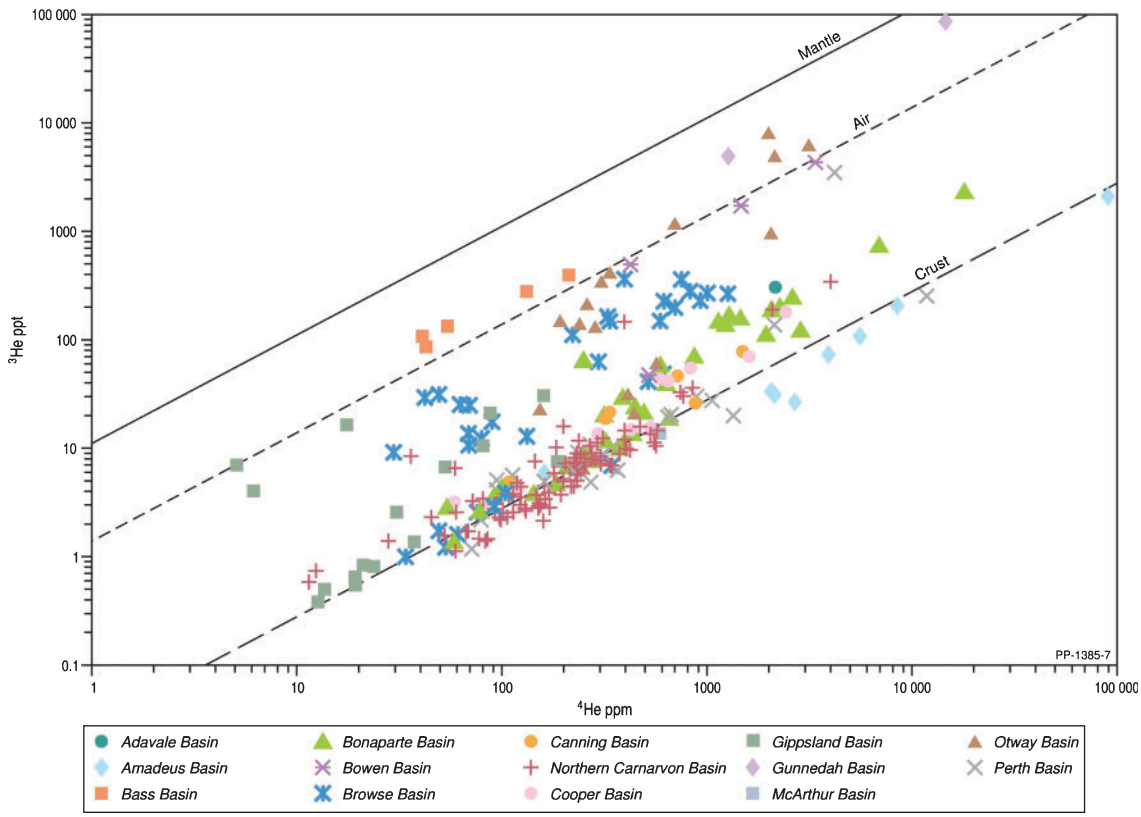

Fig. 6. Plot of ^{4}He concentration in parts per million (ppm) versus ^{3}He concentration in parts per trillion (ppt) by volume (measured by mass spectrometry (MS)). Gradient lines follow commonly used values for crust, air and mantle with $(^{3}He_{sample}/^{4}He_{sample})/(^{3}He_{air}/^{4}He_{air})$. (R/Ra) = 0.02, 1 and 8, respectively.

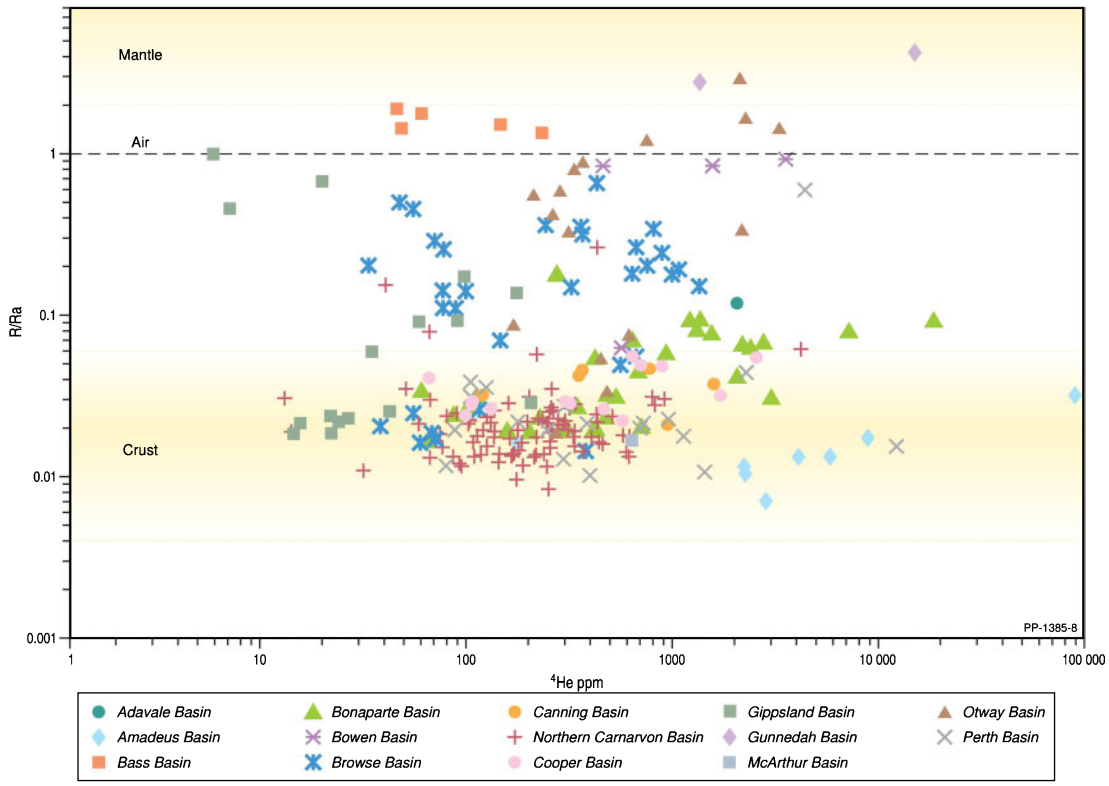

Fig. 7. Plot of ^{4}He concentration (ppm) versus the R/Ra ratio. Shaded areas show commonly accepted ranges for crustal (R/Ra 0.05 to < 0.01; Ni *et al.* 2014; and references therein) and mantle (R/Ra ~2 to 8; Darrah *et al.* 2015) sources in natural gases.

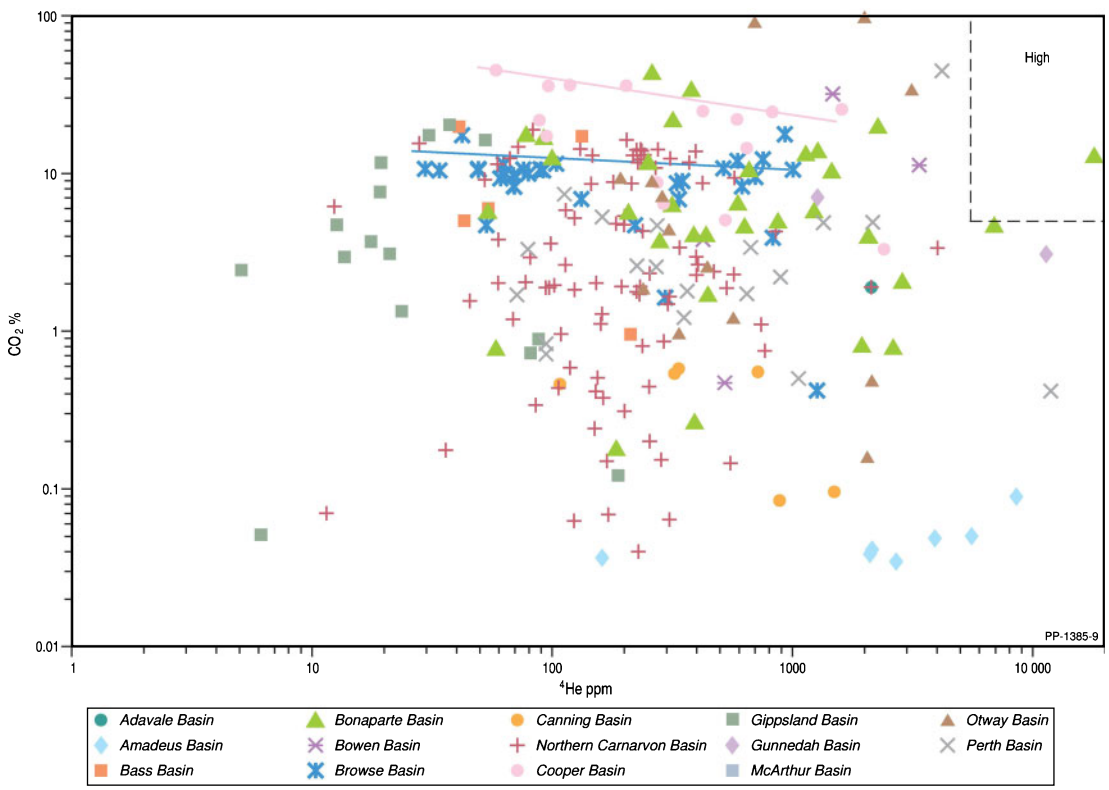

Fig. 8. Plot of ^{4}He concentration (ppm) from MS data versus carbon dioxide concentration (CO_2%) from GC data. Dotted lines represent cut-offs for high helium (>0.5%) and high carbon dioxide (>5%; Xu *et al.* 1991).

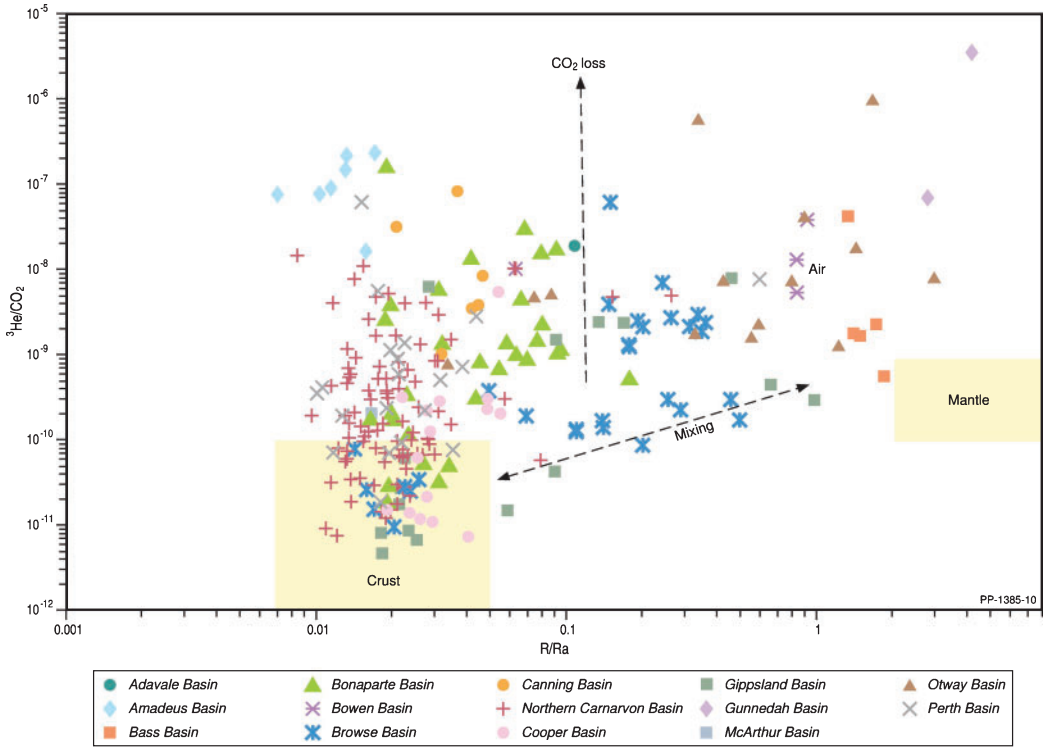

Fig. 9. Plot of R/Ra ratio versus $^{3}He/CO_2$. Shaded areas show overlap with accepted ratios for crustal and mantle sources. Magmatic $^{3}He/CO_2$ range from Gilfillan *et al*. (2008).

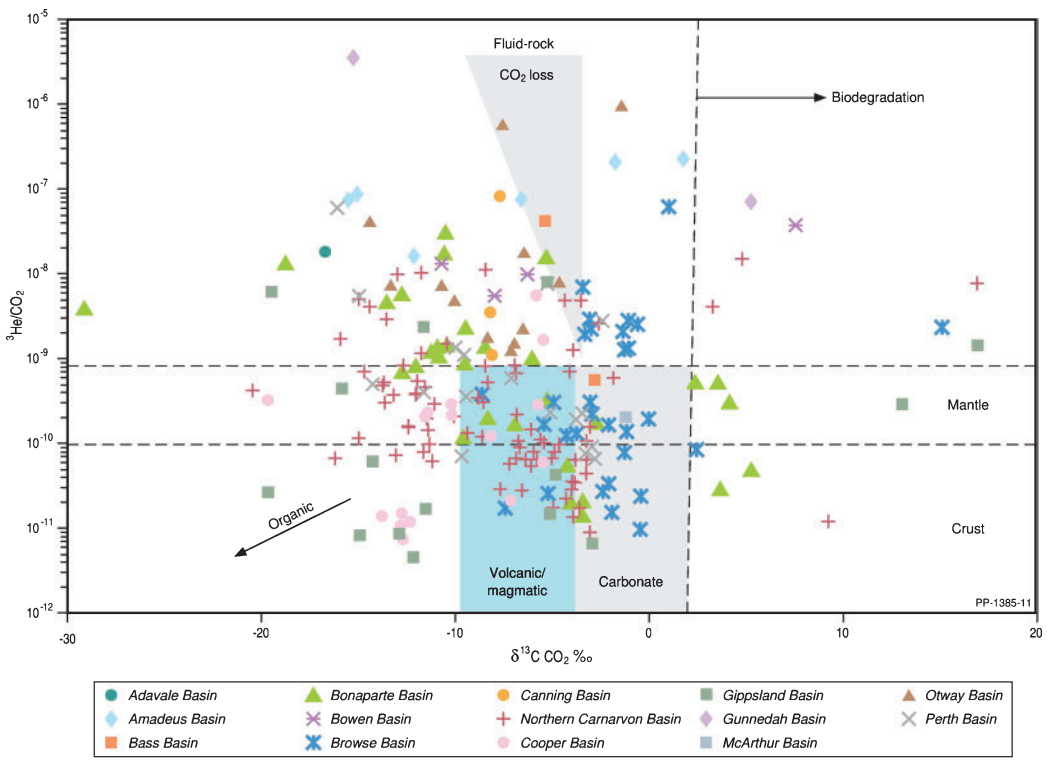

Fig. 10. Plot of carbon isotopic composition ($\delta^{13}C$) of CO_2 (‰) versus $^{3}He/CO_2$ ratio. Shaded rectangles show overlap of accepted ratios for carbon isotope of volcanic/magmatic and carbonate sources. Organic sources of CO_2 are generally depleted in ^{13}C while methanogenic enrichment in ^{13}C is associated with biodegraded gases (Boreham *et al*. 2001; Milkov 2011). The shaded triangle shows the loss of CO_2 through dissolution or leakage with little to no change in the carbon isotopes and fluid-rock interaction leading to carbonate precipitation and the depletion in ^{13}C of the smaller pool of the residual CO_2 (Snyder *et al*. 2001).

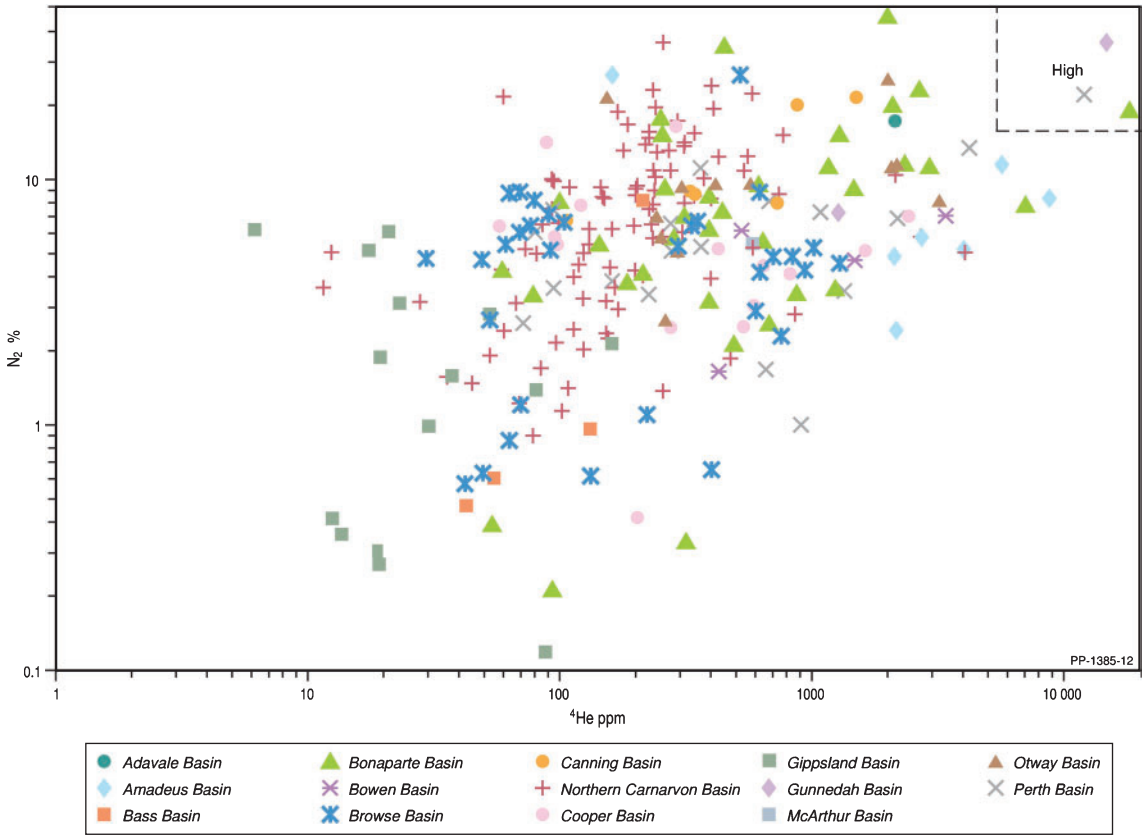

Fig. 11. Plot of ^{4}He concentration (ppm) versus nitrogen concentration (N_2%) from MS data. Dotted lines represent cut-offs for high helium (>0.5%) and high nitrogen (>15%; Xu *et al*. 1991).

gas accumulations. Relatively long (many 100 Ma) residence times (Polyak and Tolstikhin 1985) allows for significant dilution of mantle ^{3}He by radiogenic ^{4}He, making discerning mantle signatures more difficult. Despite this, some gas samples do indicate a mantle helium component with R/Ra ratios higher than a sole crustal source (Figs 6 and 7). However, gases with $0.05 < R/Ra < 1$ could be a complex mixture between radiogenic-, air- and mantle-derived sources but require further source resolution using integration with higher noble gas isotopes (Byrne *et al.* 2017; and references therein). Browse Basin natural gases with $R/Ra < 0.05$ are likely to be entirely radiogenic in origin, while some of the highest R/Ra ratios (up to 0.5 Ra) are likely a mix between air and radiogenic sources, with little to no mantle input (Main *et al*. 2014).

Relationships between helium and other inorganic gases

Tongish (1980) found that for USA gases, the highest helium concentrations were found in Paleozoic rocks at depths > 9000 ft (>2743.2 m) and associated elevated inorganic gas contents (>30% nitrogen, <30% carbon dioxide and >0.3% argon). The next section explores these compositional relationships between helium and inorganic components in the Australian natural gases.

Carbon dioxide

Although carbon dioxide is removed in the initial LNG process, its concentration in the natural gas will dilute the helium content and it may determine whether or not the natural gas is economic for LNG. Plotting helium versus carbon dioxide concentrations (Fig. 8) reveals complex associations that need to be considered on a basin-by-basin basis. For the Browse and Cooper basins, there is a weak trend of decreasing ^{4}He with increasing carbon dioxide content, suggesting that the carbon dioxide simply acts as a diluent in the reservoir. For the Northern Carnarvon Basin, a 10-fold range in helium (0.01–0.1%) occurs in association with a very wide 400-fold range in carbon dioxide (0.04–16%), indicating a non-association. In the Amadeus Basin, the helium content varies more widely from 0.016% to 0.86% with little change in the low (<0.1%) carbon dioxide content, indicating a non-association. Even at Mt Kitty-1 (Amadeus Basin), where the helium content is 9%, the CO_2 content is only slightly higher at 0.17% with the CO_2 content likely buffered by precipitation of carbonate minerals (McInnes *et al*. 2017). The highest Australian concentration of helium is found within the Late Proterozoic (Ediacaran) reservoirs of the Amadeus Basin that are below effective carbonate/evaporite seals (Clarke *et al*. 2014; McInnes *et al*. 2017; Boreham *et al*. 2018). Only Corallina-1 (Bonaparte Basin) meets the stringent criteria for both high helium (>0.5%) and high carbon dioxide (>5%; Xu *et al*. 1991).

When the R/Ra ratio is plotted against the ^{3}He/CO_2 ratio (Fig. 9), mixing between mantle and crustal helium sources can be considered for some basins (e.g. Browse, Gippsland and Otway basins); however, carbon dioxide loss is likely to be a significant feature of Australian sedimentary basins.

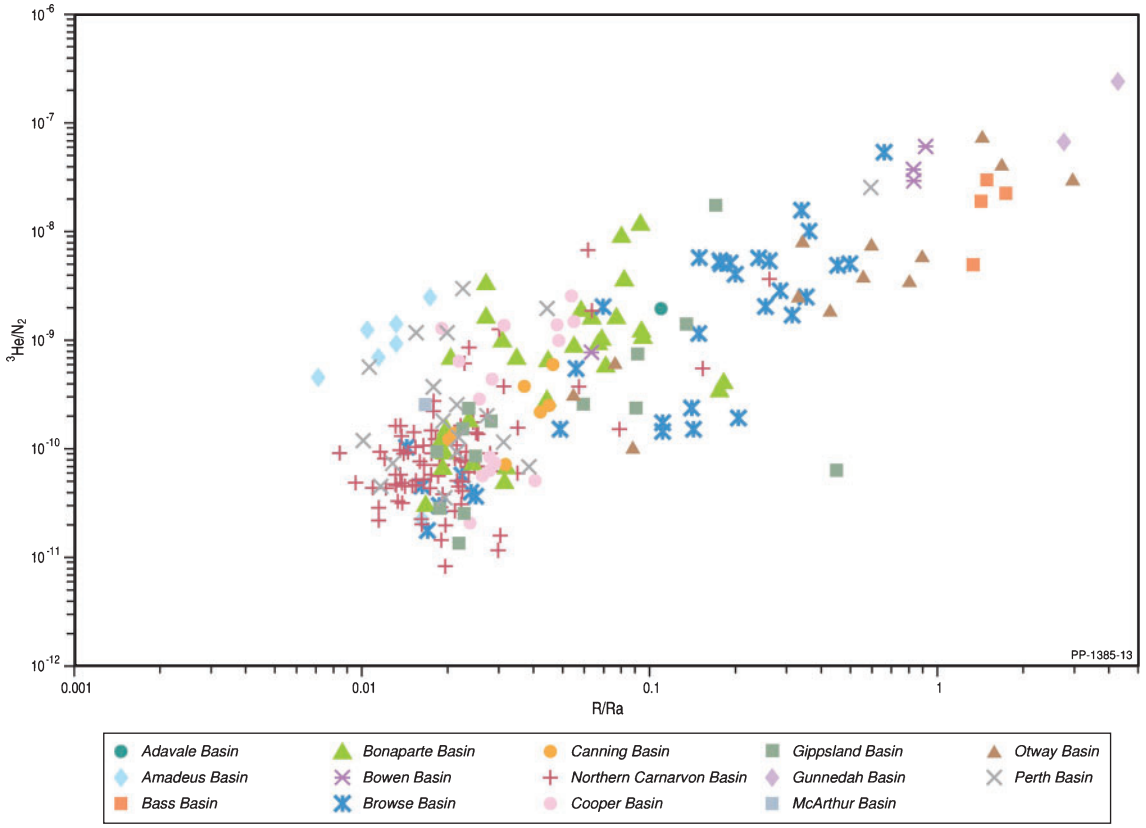

Fig. 12. Plot of R/Ra ratio versus $^3He/N_2$ ratio. Note: air is off-scale at (1, 7.13×10^{-14}).

Integration of the carbon isotope of carbon dioxide with the $^3He/CO_2$ ratio (Fig. 10) further supports the loss of carbon dioxide through either dissolution within the formation waters or carbonate precipitation associated with fluid-rock interactions and accompanying ^{13}C depletion in the residual gaseous carbon dioxide (Snyder *et al*. 2001; Watson *et al*. 2004; Tenthorey *et al*. 2011). Such depletions in $\delta^{13}C$ CO_2 (i.e. <10‰) have traditionally been attributed only to increasing organic inputs of carbon dioxide (Boreham *et al*. 2001; Milkov 2011).

Nitrogen

Natural gas samples are commonly thought to display a positive relationship between the presence of increasing nitrogen and helium (Ballentine and Sherwood Lollar 2002; Hunt *et al*. 2012). Unlike carbon dioxide, nitrogen remains throughout the LNG process and ends up in the tail gas. Therefore, understanding the origin and factors controlling the nitrogen content in natural gas are also important considerations. The relationship between helium and nitrogen is depicted in Fig. 11, where the highest nitrogen content of a natural gas occurs in the Bonaparte Basin (46% in Polkadot-1; even higher nitrogen contents are found in a few gases from the Otway and Cooper/Eromanga basins in a larger set of Australian natural gases from open file sources; Boreham *et al*. 2001). Only Corallina-1 (Bonaparte Basin), Wilga Park-1 (Gunnedah Basin) and Dunsborough-1 (Perth Basin) meet the stringent criteria for both high helium (>0.5%) and high nitrogen (>15%; Xu *et al*. 1991). While Ballentine and Sherwood Lollar (2002) stated that gases with $^4He > 0.1\%$ nearly always contain high nitrogen contents, the Australian natural gases generally show a weak positive correlation between ^4He and nitrogen and poor correlation within individual basins (Fig. 11), which does not support an overall strong correspondence between nitrogen and crustal, radiogenic helium nor the concept for a dominant deep metasedimentary or crystalline origin for the associated nitrogen (Jenden *et al*. 1988*a*, 1988*b*). Additionally, the stronger positive linear correlation between R/Ra and $^3He/N_2$ (Fig. 12) is more to do with ^3He being in the numerator of both ratios (the plot of ^3He versus N_2% (not shown) has a similar poor correlation as with ^4He versus N_2% (Fig. 11)) than any association of nitrogen with mantle ^3He.

Given that the atmospheric nitrogen content and its N-isotopic compositions ($\delta^{15}N$ N_2) have remained conservative for the past 4 Ga (Tolstikhin and Marty 1998), the complementary isotopic composition of nitrogen is a powerful tool in the attribution of organic, inorganic and mixed sources of nitrogen in natural gases (Liu *et al*. 2016; and references therein). Although the majority of gases shown in Fig. 13 do not have accompanying noble gas isotope data, they are part of the larger Australian gas dataset plotted in Fig. 5, and the overall trends are considered to reflect the basin's nitrogen isotope systematics. When plotting the nitrogen isotopic composition ($\delta^{15}N$) of nitrogen versus the nitrogen concentration (Fig. 13*a*) for the Australian-wide selection of natural gases, the data show a relatively narrow range in $\delta^{15}N$ N_2 from –7.4‰ to 2.3‰, considering the 70‰ range seen globally (Liu *et al*. 2016; and references therein). It is apparent

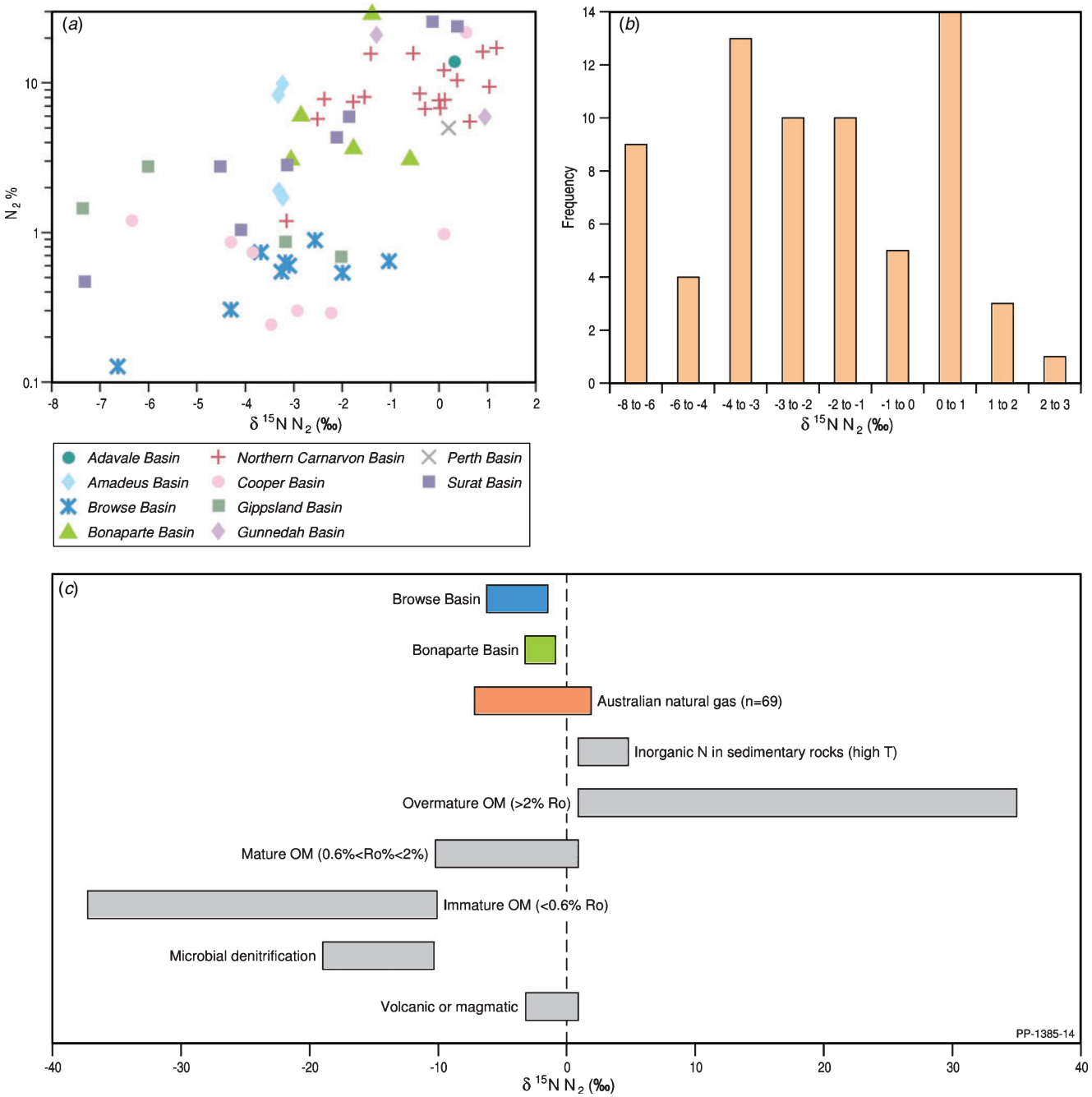

Fig. 13. Plot of (*a*) nitrogen isotopes ($\delta^{15}N$) of N_2 (‰) versus N_2 concentration (%), (*b*) frequency plot of the $\delta^{15}N$ values and (*c*) the range in different organic and inorganic nitrogen sources (modified from Liu *et al*. 2016). OM = organic matter.

from the frequency plot of the $\delta^{15}N$ N_2 values (Fig. 13*b*) that the source for nitrogen is consistent with a thermogenic origin from mature organic matter (organic N) and/or thermal decomposition of ammonium-bearing minerals (inorganic N). However, the highest frequency at 0−1‰ suggests a major atmospheric nitrogen input (Fig. 13*c*).

Neon and argon

The third major helium source input from air has not been thoroughly explored in the above discussion. To further investigate the contribution of atmospheric inputs from either air trapped in the unconsolidated sediments during deposition and/or contact of the natural gas with formation water during migration to and within the reservoir rocks, the two higher noble gases, neon (Ne) and argon (Ar), were analysed. The measured $^4He/^{20}Ne$ ratios range from 0.9 in Dory-1 (Gippsland Basin) up to > 100 000 in Big Lake-38 (Cooper Basin), with all the gases being significantly above the air ratio 0.32, indicating that helium in most samples is dominated by non-atmospheric sources. The stable isotopes of neon and argon solely of atmospheric origin are ^{20}Ne and ^{36}Ar. For

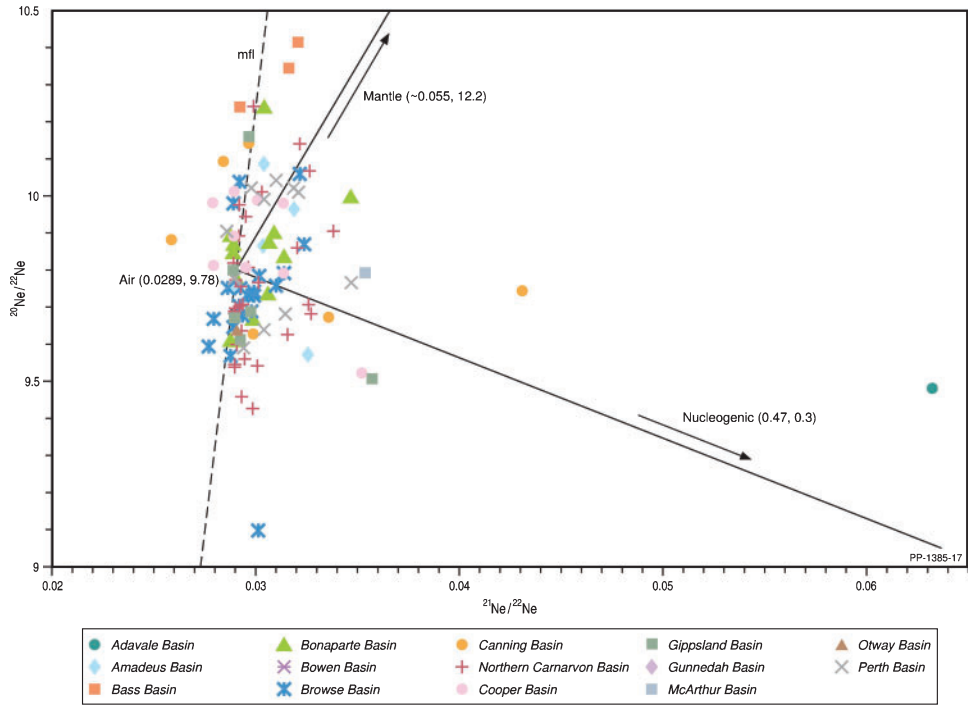

Fig. 14. Neon isotope ratio plot of $^{21}Ne/^{22}Ne$ ratio versus $^{20}Ne/^{22}Ne$ ratio. End-member values for mantle, air and crustal (nucleogenic) are sourced from Kotarba *et al*. (2014) and references therein. Crustal neon isotope distribution is controlled by nucleogenic reactions of an α particle (α) or neutron (n) (from the radioactive decay of U and Th) with isotopes of F, O, Na and Mg and the nuclear ejection of a n or α or proton (p) or positron (B^+) (Ballentine and Burnard 2002; and references therein). The mantle's neon isotopic composition likely reflects the primitive Earth's atmosphere, although the reason for the excess ^{20}Ne and ^{21}Ne is yet to be fully explained (Sarda *et al*. 1988). Mass fractionation line (mfl) refers to the mean mass-dependent fractionation corresponding to neon fractionation during fluid migration where it evolves along the dotted line (Poreda and Radicati di Brozolo 1984; Sarda *et al*. 1988).

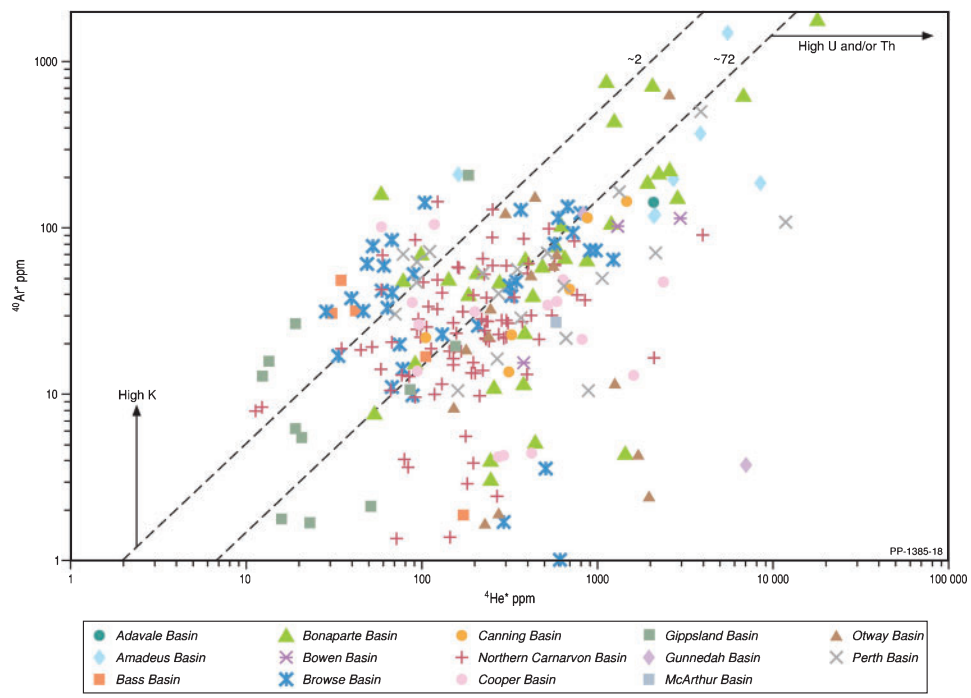

Fig. 15. Plot of radiogenic ^4He ($^4He^*$) versus radiogenic ^{40}Ar ($^{40}Ar^*$). $^4He^* = {}^4He_{total} \times (1.12 \times 10^{-5} - (^3He/^4He)_{sample})/(1.12 \times 10^{-5} - 2.8 \times 10^{-8})$ cm^3 STP (1.12×10^{-5} and 2.8×10^{-8} are the ^3He contents of mantle and crustal sources ($^3He_{air} = 1.39 \times 10^{-6}$), respectively, relative to ^4He), and $^{40}Ar^* = {}^{40}Ar_{total} \times (1–295.5/(^{40}Ar/^{36}Ar_{sample}))$ cm^3 STP (Ballentine *et al*. 1991). Gradient lines follow predicted concentrations of $^4He^*$ and $^{40}Ar^*$ from average values of U and Th, and K, respectively, from continental rocks for gas accumulation through various timescales from when the Earth was formed 4.5 Ga ago (Zartman *et al*. 1961).

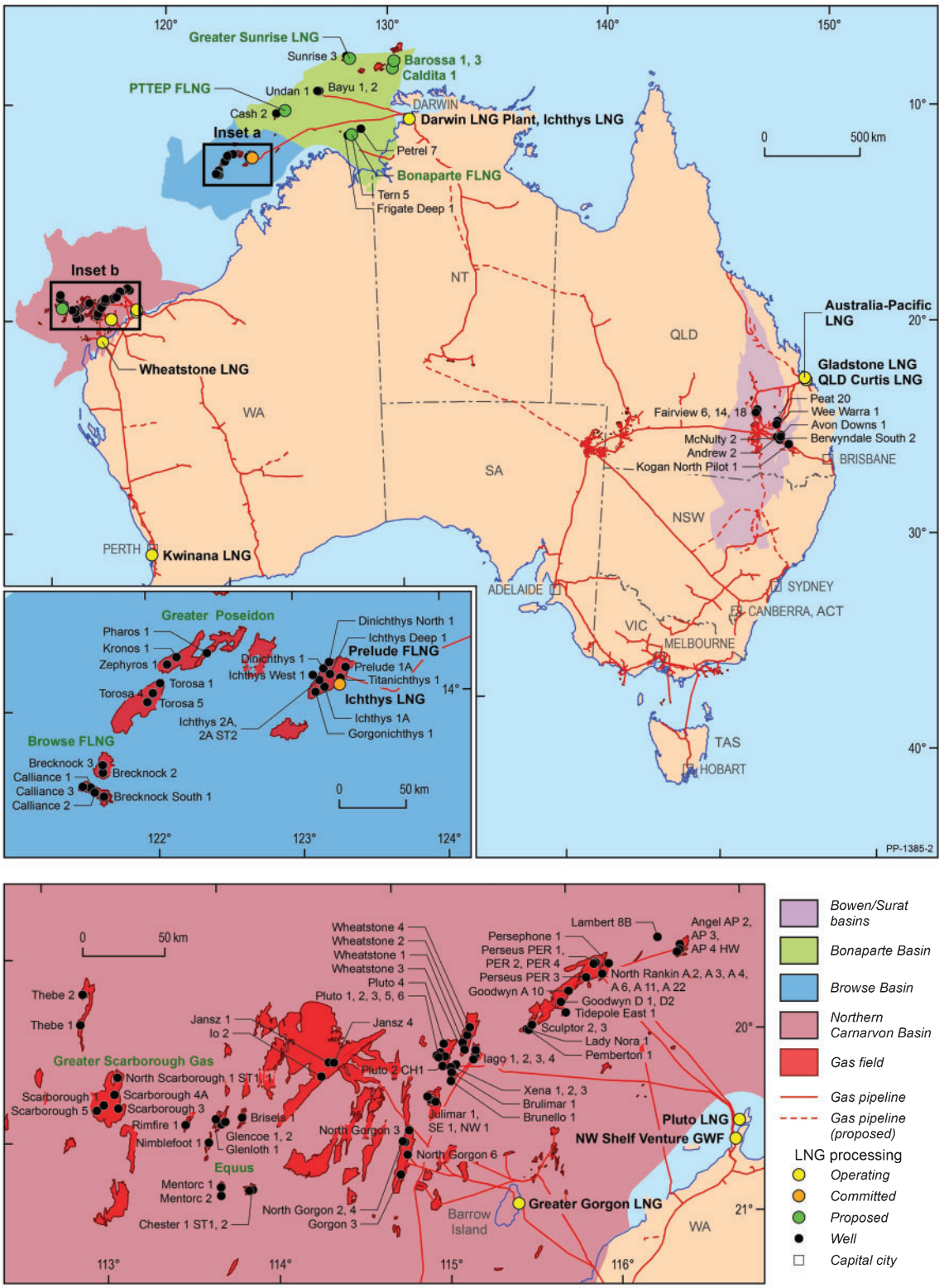

Pipelines are provided by Encom GPinfo, a Datamine Australia Pty Ltd. Whilst all care is taken in the compilation of the petroleum pipelines by Datamine, no warranty is provided re the accuracy or completeness of the information, and it is the responsibility of the Customer to ensure, by independent means, that those parts of the information used by it are correct before any reliance is placed on them. Accurate at August 2017.

Fig. 16. Location map of LNG operating, committed and proposed plants together with outlines of gas accumulations and wells therein that are used to provide average He % and average N_2% in Table 3.

Table 2. Summary of operating, committed and proposed Australian LNG developments with estimated remaining resources

Field/LNG	Co. (operator)	Gas samples at Geoscience Australia	Onshore facility	Remaining resources (Bcf[A])
LNG development east coast				
Gladstone LNG	Santos	Fairview-6, 16, 18	Gladstone	6500[1]
Qld Curtis LNG	QGC/BG/Shell	Berwyndale Sth-2, Wee Warra-1, Avon Downs-1, Kogan Nth pilot, McNulty-2, Andrew-2	Gladstone	26 600[1]
Australian Pacific LNG	ConocoPhillips		Gladstone	15 600[1,2]
LNG development west coast (N to S)				
Bayu-Undan/Darwin LNG	ConocoPhillips	Bayu-1, 2, Undan-1	Darwin LNG	1801[3]
Ichthys LNG	Inpex	Dinichthys Nth-1, Gorgonichthys-1, Ichthys-1A, 2A ST1, Ichthys West-1, Titanichthys-1		12 335[4]
Prelude FLNG	Shell	Prelude-1A, Concerto 1 ST1, Mimia-1		3469[4]
North West Shelf Venture Great Western Flank (GWF)	Woodside	Goodwyn GDA 01, 02, Lady Nora-1, Lambert-8B, North Rankin-A2 to 4, A6, A11, A22, Persephone 1, Perseus PER 01, 02 ST1, 03 ST1, 04, Sculpture-1, 2, 3, Tidepole East-1	Karratha Gas Plant	11 821[5]
Wheatstone LNG	Chevron	Julimar-1, Julimar NW-1, Julimar SE-1, Brulimar-1, Iago 1, 2, 3, 5, Wheatstone-1, 2, 3, 4	Ashburton North Gas Plant, Onslow	6818[4]
Pluto LNG	Woodside	Pluto-1 to 6, Xena-1, 2, 3	Burrup Park (Pluto) LNG Project, Karratha	4515[5]
Greater Gorgon LNG	Chevron	Io-2, Jansz-1, 4, Gorgon-3, Nth Gorgon-2, 3, 4, 6	Barrow Island	25 000[4]
LNG potential development				
Barossa-Caldita	ConocoPhillips	Barossa-1,3, Caldita-1	Darwin LNG	4300[6]
Greater Sunrise LNG	Woodside	Sunset-1, Sunset West-1, Sunrise-3		7700[7]
PTTEP FLNG	PTTEP	Cash-2		3500[8]
Bonaparte FLNG	Engie	Frigate Deep-1, Petrel-7, Tern-5		2690[9]
Greater Poseidon	ConocoPhillips, Santos	Pharos-1, Boreas-1, Poseidon Nth-1, Kronos-1, Zephyros-1		4000[10]
Greater Browse LNG	Woodside	Brecknock-2, 3, Brecknock Sth-1, Calliance-1, 2, 3, Torosa-1, 4, 5		15 951[11]
Greater Scarborough Gas	Esso Australia	Scarborough-3, 4A, Thebe-1, 2		8700[12]
Equus	Hess	Rimfire-1, Glencoe 1, 2, Briseis 1		2000[10]

[A]Remaining resources = ultimate recoverable – cumulative production = reserves (2P) + contingent resources (2C); 1 PJ = 1 Bcf; 35.315 Bcf = 1 Bm^3

[1]COAG Energy Council (2016).

[2]Origin Energy (2016).

[3]Offshore Technology (2016).

[4]EnergyQuest (2016).

[5]EnergyQuest (2016) Production is estimated from Woodside Annual Reports.

[6]Santos (2017).

[7]JPDA Production (2017).

[8]Bangkok Post (2017).

[9]Engie (2017).

[10]EnergyQuest (2017).

[11]Woodside (2016*a*). 'Greater Browse' comprises the Brecknock, Calliance and Torosa fields. For the Browse FLNG development, the reference point is defined as the outlet of the FLNG facility, which means contingent resources are reported excluding the fuel and flare required for production and processing up to the reference point. (Note: the remaining resources are calculated based on Woodside's interests to these fields of 30.6%.)

[12]Woodside (2016*b*).

Table 3. Summary of gas field average He, N_2 and CO_2 contents, estimated LNG tail gas He% and ranking from 1 to 18 of LNG projects in Table 2

*No. of samples ≥no. of well in Table 2 due to multiple tests in a single well

Development (reservoir)	Basin	No. of samples*	N_2%[A]	CO_2%[A]	He%[A]	N_2/He	He resource Bcf[B]	He tail %[C]	HLRVU[D] ranking	HRVU[E] ranking
LNG development east coast										
Gladstone LNG	Bowen/Surat	3	2.72 (0.85)	0.10 (0.04)	0.045 (0.05)	60.0	2.94	1.59	8	6
Qld Curtis LNG (QCLNG)	Bowen/Surat	7	2.79 (1.94)	0.56 (0.41)	0.025 (0.015)	112.2	6.62	0.86	7	5
Australian Pacific LNG (APLNG)	Bowen/Surat		2.79[F]		0.025[F]		3.90	0.86	10	7
LNG development west coast (N to S)										
Bayu-Undan (Elang)	Bonaparte	3	3.66 (0.26)	5.81 (0.15)	0.128 (0.07)	28.6	4.35[G]	3.28	3	2
Barossa, Caldita (*Plover*)[H]	Bonaparte	4	0.13 (0.10)	15.48 (3.98)	0.017 (0.003)	7.6	0.73	11.22	6	16
Ichthys LNG	Browse		0.55		0.051	10.8	6.26	8.23	2	3
Ichthys (*Brewster Mbr*)		13	0.56 (0.10)	9.66 (0.89)	0.058 (0.42)	9.6				
Ichthys (*Plover*)		6	0.62 (0.08)	17.12 (0.81)	0.057 (0.057)	11.0				
Prelude (*Brewster Mbr + Plover*)	Browse	3	0.30 (0.18)	10.22 (0.94)	0.028 (0.013)	10.4	0.99	8.51	5	12
North West Shelf Venture GWF (*Mungaroo*)	Northern Carnarvon	26	1.10 (0.55)	2.90 (1.12)	0.038 (0.027)	29.3	4.45	3.20	4	4
Wheatstone	Northern Carnarvon		9.91		0.021	471.9	1.43	0.21	17	11
Wheatstone (Iago, *Mungaroo*)		16	6.69 (0.85)	2.10 (0.69)	0.021 (0.006)	323.6				
Julimar (*Mungaroo*)		8	16.34 (0.43)	3.71 (1.55)	0.022 (0.006)	752.0				
Pluto (*Mungaroo*)	Northern Carnarvon	21	7.80 (1.09)	1.92 (0.6)	0.023 (0.004)	339.0	1.04	0.29	16	15
Greater Gorgon	Northern Carnarvon		2.56		0.013	196.9	3.25	0.49	13	10
Gorgon (*Mungaroo*)		27	2.52 (1.64)	13.05 (2.0)	0.016 (0.013)	152.5				
Io (*Jansz Sandstone*)		1	2.82	0.31	0.015	189.0				
Janz (*Jansz Sandstone*)		5	2.74 (0.36)	0.14 (0.02)	0.013	210.7				
LNG potential development										
Greater Sunrise *LNG* (*Plover*)	Bonaparte/Sahul	5	3.43 (1.18)	4.96 (0.55)	0.21 (0.01)	16.5	16.01	5.55	1	1
PTTEP FLNG (*Plover*)	Bonaparte/Vulcan	1	0.93	12.65	0.028	32.8	0.99	2.87	11	13
Bonaparte FLNG (*Kinmore Gp*)	Bonaparte/Petrel	7	2.88 (1.19)	1.60 (1.1)	0.054 (0.014)	53.0	1.46	1.80	12	8
Greater Poseidon (*Plover*)	Browse	8	0.48 (0.28)	12.51 (3.48)	0.010 (0.003)	49.3	0.39	1.93	15	17
Greater Browse (*Plover*)	Browse	20	0.53 (0.32)	9.44 (2.68)	0.012 (0.005)	42.6	1.98	2.23	9	14
Greater Scarborough Gas (*Barrow Group*)	N. Carnarvon/ Exmouth Plateau	9	4.35 (0.85)	0.05 (0.05)	0.025 (0.008)	173.7	2.18	0.56	14	9

Equus	N. Carnarvon/Exmouth Plateau		2.28		0.011	207.3	0.22	0.47	18	18
Mentorc (*Lower Barrow Gp*)		3	6.46 (0.07)	0.34 (0.01)	0.007 (0.002)	900.6				
Chester, Glencoe (*Murat Siltst, Jansz Sst, Mungaroo*)		18	1.59 (0.97)	2.23 (1.87)	0.012 (0.003)	136.6				

[A]Average (standard deviation).
[B]Remaining resources (Table 2) × average He %/100; 35.315 Bcf = 1 Bm^3 (1000 MMm^3).
[C]He% in the tail gas with 3% methane and the balance N_2 (https://linde-kryotechnik.ch/en/inauguration-of-first-helium-purification-liquefaction-plant-of-the-southern-hemisphere-at-darwin-australia. Verified 8 November 2017); 3% methane confirmed by the analysis of tail gas from two onshore LNG processing plants.
[D]HLRVU (helium LNG resource value unit) = remaining resource (Bcf) (Table 2) × (average He %) × (average He tail %).
[E]HRVU (helium resource value unit) = remaining resource (Bcf) (Table 2) × (average He %)^2 (Cook 1979).
[F]Assumed same as Qld Curtis LNG.
[G]Based on ultimate recoverable natural gas of 3.4 Tcf (Offshore Technology 2016).
[H]Projected production in 2023 (Offshore Technology 2016).

neon, there are distinct stable isotopic compositions for air, mantle and crustal sources, and their respective end-member neon isotope ratio values are displayed in Fig. 14. For the Australian natural gases, neon is universally dominated by an atmospheric origin with minor input from nucleogenic (crustal) neon (Ballentine 1997; and references therein) (Gilmore 4A natural gas from the Adavale Basin has the highest subordinate nucleogenic input), regardless of the basin and reservoir age from the Paleo−Mesoproterozoic (McArthur Basin) to the Cenozoic (Bass Basin). Additionally, the neon isotope systematics also mainly cluster along the mean fraction line (mfl; Fig. 14), suggesting a strong control by physical migration isotopic fractionation (Sarda *et al*. 1988 and references therein).

In air, the $^{40}Ar/^{36}Ar$ ratio is a constant 295.5 (Ballentine *et al*. 1991). Thus, the anticipated $^{40}Ar_{air}$ content can be calculated from the ^{36}Ar content, which further allows quantification of any additional radiogenic source of ^{40}Ar ($^{40}Ar^*$) produced by the radioactive decay of ^{40}K. Hence $^{40}Ar_{total} = {}^{40}Ar_{air} + {}^{40}Ar^*$, and for natural gases with $^{40}Ar/^{36}Ar > 295.5$ (for calculation of $^{40}Ar^*$ see Fig. 15 caption), $^{40}Ar^*$ and $^{40}Ar_{air}$ can be determined. The proportion of $^{40}Ar_{air}$ in Ar_{total} varies from 100% down to <20%, the latter seen in Dingo-3 (Amadeus Basin) and Ladbroke Grove-2 (Otway Basin). Since $^{40}Ar^*$ and $^{4}He^*$ (for calculation of $^{4}He^*$ see Fig. 15 caption) are both radiogenic isotopes, their production ratio is a function of the original ratio of potassium and uranium (K/U), respectively. Fig. 15 shows the cross-plot of $^{4}He^*$ versus $^{40}Ar^*$. Although some of the natural gases plot within the predicted $^{40}Ar^*$ and $^{4}He^*$ (i.e. within the dotted lines in Fig. 15) based on average crustal concentrations of K, U and Th (Zartman *et al*. 1961), most gases in the individual Australian basins plot outside the predicted range, reflecting a disconnect between their different radioactive mineral (U/Th for $^{4}He^*$ and K for $^{40}Ar^*$) sources.

The $N_2/^{40}Ar_{air}$ ratios for Australian natural gases range from around 1 to 3878, with the highest value in Dingo-3 gas, Amadeus Basin. Input of nitrogen from ASW and atmospheric sources would be expected to have values between ~37 and 83, although values two to three times higher than this are commonly observed in hydrocarbon- and CO_2-rich natural gases (Zartman *et al*. 1961), while most volcanic sources extend $N_2/^{40}Ar_{air}$ ratios to 300 (Jenden *et al*. 1988*b*). Approximately 86% of Australian natural gases have $N_2/^{40}Ar_{air}$ values <300. Therefore, while the nitrogen in Australian natural gases has a quantifiable high atmospheric input (i.e. ASW), there is notable contribution from non-atmospheric sources in many samples. The non-atmospheric sources ($N_{2excess}$) can be estimated using the formula $N_{2excess} = N_{2sample} - (^{36}Ar_{sample} \times (N_2/^{36}Ar)_{ASW})$ with $N_{2excess}$ ranging from 5% to 100% (average 79%) of total nitrogen. As a consequence, the narrower isotopic range in $\delta^{15}N$ N_2 for the Australian natural gases (Fig. 13) is partially a result of attenuation towards $\delta^{15}N$ N_{2air} (0‰) with increasing air input. Consequently, the $\delta^{15}N$ nitrogen for other contributing nitrogen sources most likely have a wider N-isotopic range and, for an organic nitrogen source, it is in accord with the wide range in gas maturities (Figs 3 and 4).

Helium from LNG processing

Ironically, helium was first extracted from LNG over a century ago with the latter being discarded for lack of market

(Flower 2012). However, not long after the value of LNG was recognised (around 80 years ago), there eventuated the opportunity to produce helium from the by-product of the cryogenic LNG process (Flower 2012). Here, the recovery efficiency of the non-condensable, helium-enriched tail gas by-product is high throughout the process of carbon dioxide removal, collection of the natural gas liquids and containment of the LNG. Pilot studies using a non-cryogenic pressure swing absorption process offer an alternative pathway, although costs are high and helium recovery efficiencies are only around 60% (Das *et al*. 2012).

In the Australian context, the locations of operating and committed/proposed LNG projects, together with their feed-in gas accumulations, are shown in Fig. 16. Based on publicly available information, remaining natural gas resources for each LNG project are listed in Table 2. The wells used to calculate the average concentrations of helium for each LNG project are also plotted in Fig. 16 and the average contents (%) of nitrogen, carbon dioxide and helium are listed in Table 3. LNG is forming an increasing proportion of Australia's total gas production; in 2016, LNG was 60.3% of the total gas production of 3437 Bcf (97.2 Bm^3) from conventional and CSG resources (Department of Environment and Energy 2017). By multiplying the remaining natural gas resources (Table 2) by the average helium percentage (Table 3), the remaining helium resources can be calculated for each LNG project (data are listed in Table 3). The summed total of the ultimate helium recovery is 59.0 Bcf (1.67 Bm^3), which is included in Fig. 1*b*, giving Australia potentially a substantial stake in global helium prospectivity. In 2015, the world's helium production was 5.51 Bcf (156 MMm^3), with only a slight drop in the 2016 estimate, and Australia's helium production was steady at 0.14 Bcf (4.0 MMm^3) (USGS 2017*b*) from the only helium extraction plant in Darwin.

Using the analysis of the co-mingled feed-in gas to the LNG plants in Darwin and Gladstone (Fig. 16), it was determined that, on average, He and N_2 are conserved throughout the LNG industrial processing. The N_2/He ratio of the co-mingled feed-in gas to the Darwin LNG plant is very similar to the N_2/He ratio of the tail gas (feed-in He = 0.1% and N_2/He = 37.3 and tail gas He = 3.0% and N_2/He = 31.1). A similar result is obtained for the LNG plant at Gladstone, in which the LNG feed-in gas has values of He = 0.017% and N_2/He = 80.2 and the tail gas has He = 1.1% and N_2/He = 87.7.

The data from the Australian LNG plants' gases compare favourably with the amount of helium and the N_2/He ratio derived from averaging the gas composition from the individual produced wells (Table 3 and Fig. 16), with Bayu-Undan averaging He = 0.13% and N_2/He = 28.6 and Gladstone averaging He = 0.03% and N_2/He = 85.7. Therefore, all other LNG examples in Table 3 are based on this 'no loss' determination with a wide range in N_2/He from 7.6 to 752 and a calculated helium content in the tail gas from 0.21% to 11.22% (in Table 3 note that the tail gas was considered to contain 3% methane as the only other component (see footnote in Table 3)). Notably, 11 of the 18 LNG projects have tail gas helium contents >1%, which is at the lower helium concentration limit for global helium processing in 2016–2017 (Linde 2017). The estimated helium enrichment factor (%He tail ÷ %He initial) ranges from a low 12.4 at Pluto in the Northern Carnarvon Basin to a very high 162 and 299 in the Browse Basin for Prelude and Ichthys, respectively, and an extremely high 660 in Barossa-Caldita, Bonaparte Basin. Interestingly, for the helium extraction plant using Qatar's North Field natural gas composition (0.04% He), the LNG helium enrichment factor is even lower at 10; however, the giant helium resource of 360 Bcf (10.2 Bm^3) more than compensates for the unfavourable chemistry (Daly 2005).

A ranking seriatim can be applied that uses the average abundance of helium (He%) in the tail gas together with the remaining helium resource volume for each LNG catchment area. Thus, a relative helium LNG resource value unit (HLRVU) is defined by the multiplication of the remaining helium resource by the He% tail gas. This is a similar approach to the relative helium resource value unit (HRVU), defined by the multiplication of the remaining helium resource by the He% initially in the natural gas (Cook 1979). The HLRVU takes into account the nitrogen content of the natural gas while HRVU does not (Table 3). From the HLRVU, the top five ranked LNG projects (Table 3) come from the Bonaparte, Browse and Northern Carnarvon basins, with the potential Greater Sunrise development (Bonaparte Basin) being ranked first, the Ichthys development (Bonaparte Basin) ranked second, followed by a near identical ranking between the producing helium extraction plant in Darwin, using the feed-in gas from the Bayu-Undan accumulation (note: the ranking is based on the ultimate recoverable) in the Bonaparte Basin, and the Goodwyn–North Rankin and tie-back accumulations of the North West Shelf Venture (note approximately half of the ultimate recoverable has already been produced) in the Northern Carnarvon Basin. The Prelude LNG is ranked fifth. When using the HRVU, it should be noted that Greater Sunrise remains on top, the Ichthys and Bayu-Undan rankings are reversed, the North West Shelf Venture is forth, while Prelude is ranked lower (Table 3). Although the Greater Sunrise accumulation does not have the highest helium resource, its greater helium content (average 0.21%), together with moderate nitrogen content, leads to its excellent HLRVU. The greater Ichthys gas accumulation has an even lower helium content (average 0.065%); however, this negative is more than compensated for by the large resource volume and low nitrogen content in the LNG feed-in gas.

The wide ranging gas compositions in different wells and formations in a given gas field (Table 3) may guide the timing of LNG development if linked with helium extraction. For example, any future input from the Barossa-Caldita gas accumulation (ConocoPhillips 2018; Fig. 16) to the Darwin LNG feed-in gas will enrich the helium content of the LNG tail gas (average helium content in the Barossa-Caldita tail gas is extremely high at 11.2% and N_2/He = 7.6; Table 3). However, the proportion of LNG tail gas derived from a Barossa-Caldita feed-in component will be lower than from a Bayu-Undan feed-in component due to the former's very low initial nitrogen content (0.203%), and together with the projected LNG production, leads to a HLRVU ranking of six for Barossa-Caldita (Table 3). Interestingly, the just completed analysis of the Ascalon-Saratoga gas accumulation (Fig. 2, inset 1d; situated between the Bayu-Undan and Ichthys offshore pipelines, Fig. 16) with a 3.2 Tcf contingent gas resource (Octanex 2017) and average helium and nitrogen

of 0.14% and 3.27% respectively, offers a future alternative feed-in gas to LNG processing in Darwin. With a calculated LNG tail-gas of 3.9% helium together with a similar 4.4 Bcf ultimate recoverable volume of helium compared to the original Bayu-Undan gas accumulation, Ascalon-Saratoga if developed should ensure longevity of downstream helium processing in Darwin. Furthermore, in the Ichthys gas field, the ~two-fold difference in carbon dioxide content between the Brewster and Plover reservoirs (Table 3) may determine the order of gas production, as it has in the Greater Gorgon development with the Jansz and Io gas accumulations containing low abundances of carbon dioxide (average $CO_2 = 0.14\%$ and 0.31%, respectively; Table 3), supplying the early LNG trains in the Barrow Island LNG facility followed later by the 'Gorgon' gas fields with high carbon dioxide content (average $CO_2 = 13\%$; Table 3).

Helium resource potential should also be considered for gas accumulations that service the domestic market, which uses ~40% of the total natural gas production (Department of Environment and Energy 2017). As an example, the offshore Blacktip gas accumulation (Fig. 2) in the southern Bonaparte Basin supplies gas to the Northern Territory via an onshore gas processing plant (ENI 2018). With helium and nitrogen contents of 0.060% and 9.18% respectively, giving a calculated tail gas of 0.63% helium, and together with a gas reserve of 1.2 Tcf (Oil&Gas Journal 2009) it slots into Table 3 with a HLRVU in 16th place.

A further understanding of the origin and distribution of helium in Australian basins is still required to enable an assessment of whether helium can play a bigger role in the upstream and downstream gas economy where conservation is encouraged and emissions are reduced. Simply collecting LNG tail gas may not be economic in the short-term, but a collective commitment to conserve helium resources would be an investment in the future. For example, a common storage repository for tail gas from LNG and domestic gas projects with additional helium upgrading may achieve higher helium concentrations in Australia, such as recorded at Qatar I/II (29%) and at the USA's BLM Cliffside helium reserve (32%) (Table 1), and hence, become more attractive for further exploitation.

Conclusions

Helium in Australian natural gases is generally dominated by crustal sources with the older (Late Paleozoic−Proterozoic) reservoirs commonly having the highest crustal ^4He input. Natural gases with the highest ^3He inputs are concentrated in eastern Australia in direct response to younger tectonic/magmatic events. The concentration of helium is linked with the sealing efficiency of the reservoir with evaporitic rocks forming the most competent seals resulting in high helium concentrations. However, this is moderated by the input of large volumes of natural gas from primary and secondary cracking reactions over a wide maturity range, resulting in Australian natural gases generally having low helium (<0.1%) contents. Helium is not generally source-associated with inorganic carbon dioxide and nitrogen gases, with the latter having a significant source input from ancient air-saturated water.

Current and future LNG projects across Australia offer the opportunity to deliver a helium-enriched by-product suitable for economic exploitation through downstream helium extraction. Additionally, natural gas for domestic use also provides a yet to be tapped helium extraction potential. Australia has large volumes of processed natural gas containing variable helium concentrations, with many above the lower limit of 0.04% helium in the raw gas used for helium extraction in other parts of the world. This study has shown that there is no significant loss of helium and nitrogen throughout the LNG process. This, together with estimated natural gas field remaining resources, resulted in a helium volumetric analysis whereby the Greater Sunrise (Bonaparte Basin), Ichthys (Browse Basin) and Goodwyn–North Rankin North West Shelf Venture (Northern Carnarvon Basin) gas accumulations potentially have a higher untapped value in helium extraction (i.e. resulting from current and future LNG production) compared with Australia's sole commercial onshore helium extraction facility in Darwin, based on Bayu-Undan (Bonaparte Basin) natural gas. Of particular importance is that 14 of the 18 current and proposed/potential LNG projects also offer a helium-rich tail gas (>0.5% He) that could be considered suitable for helium extraction with appropriate technologies and economic environment for onshore and/or offshore helium production facilities. Hence, Australia has the potential for significant growth in the extraction of helium from natural gas to provide a reliable supply of this critical commodity now and into the future.

Conflicts of interest

No conflicts of interest exist between these authors and any other person or organisation.

Acknowledgements

The authors of this work would like to thank Silvio Mezzomo, Bianca Reece and Chris Evenden for figure production. Tom Bernecker, Amber Jarrett and Jennie Totterdell are thanked for their internal peer-reviews. The collective technical staff of the Isotope and Organic Geochemistry Laboratory at Geoscience Australia (Junhong Chen, Ziqing Hong, Neel Jinadasa, Prince Palatty and Jacob Sohn) and previous staff members (Janet Hope and Zoltan Horvath) are recognised for their analytical expertise and gas data over the past two decades. Tamara Buckler and the Resources Division Information Services Data Management Team are acknowledged for their management of the Geoscience Australia databases. This work was only possible with the support of the petroleum exploration companies, in conjunction with the states/territory geological surveys, who provided the Australian natural gases, and in some cases, resampled from the well head for this study. Andrew Murray and an anonymous reviewer are thanked for their thoughtful reviews and Steve Mackie and Emma Proudlock for their editorial efforts. The Geoscience Australia authors publish with the permission of the CEO, Geoscience Australia

References

Aali, J., Rahimpour-Bonab, H., and Kamali, M. R. (2006). Geochemistry and origin of the world's largest gas field from Persian Gulf, Iran. *Journal of Petroleum Science Engineering* **50**, 161–175. doi:10.1016/j.petrol.2005.12.004

Allègre, C. J., Staudacher, T., and Sarda, P. (1987). Rare gas systematics: formation of the atmosphere, evolution and structure of Earth's mantle.

Earth and Planetary Science Letters **81**, 127–150. doi:10.1016/0012-821X(87)90151-8

Alvarez, L. W., and Cornog, R. (1939). He^3 in helium. *Physical Review* **56**, 379. doi:10.1103/PhysRev.56.379.2

American Chemical Society National Historic Chemical Landmarks (2000). Discovery of Helium in Natural Gas. Available at: http://www.acs.org/content/acs/en/education/whatischemistry/landmarks/heliumnaturalgas.html [Verified 28 November 2017]

Australian Energy Resources Assessment (AERA) (2016). Available at http://www.ga.gov.au/aera/gas [Verified 8 November 2017].

Australian Production and Petroleum Exploration Association (APPEA) (2017). Australian LNG projects. Available at https://www.appea.com.au/oil-gas-explained/operation/australian-lng-projects/ [Verified 8 November 2017].

Ballentine, C. J. (1997). Resolving the mantle He/Ne and crustal $^{21}Ne/^{22}Ne$ in well gases. *Earth and Planetary Science Letters* **152**, 233–249. doi:10.1016/S0012-821X(97)00142-8

Ballentine, C. J., and Burnard, P. G. (2002). Production, release and transport of noble gases in the continental crust. *Reviews in Mineralogy and Geochemistry* **47**, 481–538. doi:10.2138/rmg.2002.47.12

Ballentine, C. J., and Sherwood Lollar, B. (2002). Regional groundwater focussing of nitrogen and noble gases into the Hugoton-Panhandle giant gas field, USA. *Geochimica et Cosmochimica Acta* **66**, 2483–2497. doi:10.1016/S0016-7037(02)00850-5

Ballentine, C. J., O'Nions, R. K., Oxburgh, E. R., Horvath, F., and Deak, J. (1991). Rare gas constraints on hydrocarbon accumulation, crustal degassing and groundwater flow in the Pannonian Basin. *Earth and Planetary Science Letters* **105**, 229–246. doi:10.1016/0012-821X(91)90133-3

Baly, E. C. C. (1898). Helium in the atmosphere. *Nature* **58**, 545. doi:10.1038/058545a0

Bangkok Post (2017). PTTEP scouting Timor Sea to share LNG equipment, Bangkok Post 23 May 2017 https://www.pressreader.com/thailand/bangkok-post/20170523/281981787529049 [Verified 28 November 2017).

Boote, D. R. D., Clark-Lowes, D. D., and Traut, M. W. (1998). Palaeozoic petroleum systems of North Africa. *Geological Society, London, Special Publications* **132**, 7–68. doi:10.1144/GSL.SP.1998.132.01.02

Boreham, C. J., and Edwards, D. S. (2008). Abundance and carbon isotopic composition of *neo*-pentane in Australian natural gases. *Organic Geochemistry* **39**, 550–566. doi:10.1016/j.orggeochem.2007.11.004

Boreham, C. J., Hope, J. M., and Hartung-Kagi, B. (2001). Understanding source, distribution and preservation of Australian natural gas: a geochemical perspective. *The APPEA Journal* **41**(1), 523–547. doi:10.1071/AJ00026

Boreham, C., Edwards, D., Poreda, R., and Henson, P. (2017). Origin and use of helium in Australian natural gases. In '28th International Meeting on Organic Geochemistry (IMOG), Florence, Italy, 17–22 September 2017'. Unpublished Abstract. Available at http://imog2017.org/wp-content/uploads/2017/04/032.pdf. [Verified 8 November 2017].

Boreham, C. J., Edwards, D. S., Jarrett, A., Davies, J., Poreda, R., Sessions, A., and Eiler, J. (2018). Gas systems of the Amadeus Basin, Australia. In '20th International Conference on Gas Geochemistry (ICGG 2018), Bangkok, Thailand, 20–21 December 2018'. Accepted Abstract. Available at http://waset.org/pdf/books/?id=82249&pageNumber=657 [Verified 28 November 2017]

Brown, A. A. (2010). Formation of high helium gases: a guide to explorationists. In 'AAPG Search and Discovery Article #90104 AAPG Annual Convention and Exhibition, New Orleans, 11–14 April 2010'. Poster available at http://www.searchanddiscovery.com/documents/2010/80115brown/poster01.pdf. [Verified 8 November 2017].

Bureau of Land Management (2017). Federal helium program: frequently asked questions. Available at: http://www.blm.gov/nm/st/en/prog/energy/helium/federal_helium_program/federal_helium_program.html [Verified 28 November 2017].

Byrne, D. J., Barry, P. H., Lawson, M., and Ballentine, C. J. (2017). Noble gases in conventional and unconventional petroleum systems. In 'From Source to Seeps: Geochemical Applications in Hydrocarbon Systems'. Special Publication, 468 (Eds M. Lawson, M.J. Formolo and J.M. Eiler) (Geological Society: London). doi:10.1144/SP468.5

Cady, H. P., and McFarland, D. F. (1907). The occurrence of helium in natural gas and the composition of natural gas. *Journal of the American Chemical Society* **29**, 1523–1536. doi:10.1021/ja01965a001

Cai, Z., Clarke, R. H., and Nuttall, W. J. (2012). Helium demand. In 'The Future of Helium as a Natural Resource'. (Eds W.J. Nuttall, R.H. Clarke and B.A. Glowacki) pp. 134–156. (Routledge: London).

Cartwright, J. (2012). Shortages spur race for helium-3 alternative. Chemistry world online, 12 January, 2012. Available at http://www.rsc.org/chemistryworld/News/2012/January/helium-3-isotopes-shortage-alternatives-neutron-detectors.asp [Verified 8 November 2017].

CERN (European Organization for Nuclear Research) 2017. The Large Hadron Collider. Available at https://home.cern/topics/large-hadron-collider/ [Verified 8 November 2017].

Chen, J., and Boreham, C. (2010). GC-IRMS analyses of natural gases and geochemical application. In '16th Australian Organic Geochemistry Conference: Program and Abstracts'. Geoscience Australia. *Record* **2010**(42), 84–85. http://pid.geoscience.gov.au/dataset/71227 [Verified 8 November 2017].

Clarke, R. H., and Clare, R. (2012). Helium from the air: the backstop. In 'The Future of Helium as a Natural Resource'. (Eds W.J. Nuttall, R.H. Clarke and B.A. Glowacki) pp. 119–133. (Routledge: London).

Clarke, R. H., Nuttall, W. L., and Glowacki, B. A. (2012). Introduction. In 'The Future of Helium as a Natural Resource'. (Eds W.J. Nuttall, R.H. Clarke and B.A. Glowacki) pp. 1–14. (Routledge: London).

Clarke, M., Seddon, D., and Ambrose, G. (2014). Helium, will it be the next mineral boom in Australia? *The AusIMM Bulletin* **6**(12), 83–85.

Class, C., and Goldstein, S. L. (2005). Evolution of helium isotopes in the Earth's mantle. *Nature* **436**, 1107–1112. doi:10.1038/nature03930

Claudet, S., Brodzinski, K., Darras, V., Delikaris, D., Duret-Bourgoz, E., Ferlin, G., and Tavian, L. (2015). Helium inventory management and losses for LHC cryogenics: strategy and results for run 1. *Physics Procedia* **67**, 66–71. doi:10.1016/j.phpro.2015.06.012

COAG Energy Council (2016). Coal seam, shale and tight gas in Australia: Resources assessment and operation overview 2016. Upstream Petroleum Resources Working Group Report to COAG, Geoscience Australia Energy Council, November 2016. 32pp. Available at http://www.coagenergycouncil.gov.au/sites/prod.energycouncil/files/publications/documents/UPR%20Unconventional%20Resources%20Report%202016_0.pdf [Verified 28 November 2017].

ConocoPhillips (2017). Darwin LNG. Available at http://www.conocophillips.com.au/our-business-activities/our-projects/Pages/darwin-lng.aspx [Verified 28 November 2017].

ConocoPhillips (2018). Barossa Project. Available at http://www.conocophillips.com.au/what-we-do/our-projects-activities/barossa-project/ [Verified 23 January 2018].

Cook, E. (1979). The helium question. *Science* **206**, 1141–1147. doi:10.1126/science.206.4423.1141

Crookes, W. (1897). Traces of helium in the water at Bath; mentioned on page 243 in Nath (2013).

Crookes, W. (1898). Helium in the atmosphere. *Nature* **58**(1511), 570. doi:10.1038/058570a0

Cull, J. P., and Conley, D. (1983). Geothermal gradients and heat flow in Australian sedimentary Basins. *BMR Journal of Australian Geology and Geophysics* **8**, 329–337.

Daly, W. J. (2005). Helium recovery from LNG. International Petroleum Technology Conference, Qatar, 21–23 November, 2005. pp. 1–4.

Available at https://www.onepetro.org/conference-paper/IPTC-10720-MS [Verified 8 November 2017].

Darrah, T. H., Tedesco, D., Tassi, F., Vaselli, O., Cuoco, E., and Poreda, R. J. (2013). Gas chemistry of the Dallol region of the Danakil Depression in the Afar region of the northern-most East African Rift. *Chemical Geology* **339**, 16–29. doi:10.1016/j.chemgeo.2012.10.036

Darrah, T. H., Vengosh, A., Jackson, R. B., Warner, N. R., and Poreda, R. J. (2014). Noble gases identify the mechanisms of fugitive gas contamination in drinking-water wells overlying the Marcellus and Barnett Shales. *Proceedings of the National Academy of Sciences of the United States of America* **111**(39), 14076–14081. doi:10.1073/pnas.1322107111

Darrah, T. H., Jackson, R. B., Vengosh, A., Warner, N. R., Whyte, C. J., Walsh, T. B., Kondash, A. J., and Poreda, R. J. (2015). The evolution of Devonian hydrocarbon gases in shallow aquifers of the northern Appalachian Basin: insights from integrating noble gas and hydrocarbon geochemistry. *Geochimica et Cosmochimica Acta* **170**, 321–355. doi:10.1016/j.gca.2015.09.006

Das, N. K., Bhandari, R. K., and Mallik, C. (2012). Harnessing helium from the Earth's interior. In 'The Future of Helium as a Natural Resource'. (Eds W.J. Nuttall, R.H. Clarke and B.A. Glowacki) pp. 101–118. (Routledge: London).

de Laeter, J. R., Böhlke, J. K., de Bièvre, P., Hidaka, H., Peiser, H. S., Rosman, K. J. R., and Kim, J. S. (2003). Atomic weights of the elements: review 2000 (IUPAC Technical Report). *Pure and Applied Chemistry* **75**, 683–800. doi:10.1351/pac200375060683

Department of Environment and Energy (2017). Australian Petroleum Statistics Issue 250, May 2017. Available at http://www.environment.gov.au/energy/petroleum-statistics [Verified 8 November 2017]

Department of Industry Innovation and Science (DIIS) (2017). Offshore Petroleum Exploration Acreage Release. Available at http://www.petroleum-acreage.gov.au/ [Verified 25 January 2018].

Energy Quest (2016) November Report. Available at http://www.energyquest.com.au/insightsandanalysis.php?typ=2&m=1&y=2016 [Verified 28 November 2017].

Energy Quest (2017) March Report. Available at http://www.energyquest.com.au/insightsandanalysis.php?id=276 [Verified 28 November 2017].

Engie (2017). Bonaparte (AU). Available at http://www.engie-ep.com/en/our-activities/development-projects/bonaparte-au.aspx [Verified 28 November 2017].

ENI (2018). The Blacktip Gas Field and the Yelcherr Gas Plant. Available at: https://www.eni.com/en_IT/media/focus-n/australia/blacktip_gas_field_yelcherr_gas_plant.page [Verified 24 February 2018].

Flower, A. (2012). The global liquefied natural gas market. In 'The Future of Helium as a Natural Resource'. (Eds W.J. Nuttall, R.H. Clarke and B.A. Glowacki) pp. 69–87. (Routledge: London).

Gage, B. D., and Driskill, D. L. (2004). 'Helium resources of The United States−2003'. U.S. Department of the Interior, Bureau of Land Management, Technical Note 415, 35pp.

Gilfillan, S. M. V., Ballentine, C. J., Holland, G., Blagburn, D., Sherwood Lollar, B., Stevens, S., Schoell, M., and Cassidy, M. (2008). The noble gas geochemistry of natural CO_2 gas reservoirs from the Colorado Plateau and Rocky Mountain Provinces, USA. *Geochimica et Cosmochimica Acta* **72**, 1174–1198. doi:10.1016/j.gca.2007.10.009

Gilfillan, S. M. V., Sherwood Lollar, B., Holland, G., Blagburn, D., Stevens, S., Schoell, M., Cassidy, M., Ding, Z., Zhou, Z., Lacrampe-Couloume, G., and Ballentine, C. J. (2009). Solubility trapping in formation water as dominant CO_2 sink in natural gas fields. *Nature* **458**(7238), 614–618. doi:10.1038/nature07852

Hamak, J.E. (2013). Helium. United States Geological Survey, Mineral Commodity Summaries 2013.

Hand, E. (2016). Massive helium fields found in Rift Zone of Tanzania. *Science* **353**, 109–110. doi:10.1126/science.353.6295.109

Harkness, J. S., Darrah, T. H., Warner, N. R., Whyte, C. J., Moore, M. T., Millot, R., Kloppmann, W., Jackson, R. B., and Vengosh, A. (2017). The geochemistry of naturally occurring methane and saline groundwater in an area of unconventional shale gas development. *Geochimica et Cosmochimica Acta* **208**, 302–334. doi:10.1016/j.gca.2017.03.039

Hasterok, D., and Gard, M. (2016). Utilizing thermal isostasy to estimate sub-lithospheric heat flow and anomalous crustal radioactivity. *Earth and Planetary Science Letters* **450**, 197–207. doi:10.1016/j.epsl.2016.06.037

Helium One (2017*a*). Announcing the maiden helium resource assessment for Helium One's Rukwa Basin Project in Tanzania. Available at http://www.helium-one.com/projects/rukwa/ [Verified 05 December 2017].

Helium One (2017*b*). Helium Demand and Market Fundamentals. Available at http://www.helium-one.com/helium/demand-market-fundamentals/ [Verified 28 November 2017].

Hooker, B. (2012). Helium in Russia. In 'The Future of Helium as a Natural Resource'. (Eds W.J. Nuttall, R.H. Clarke and B.A. Glowacki) pp. 88–100. (Routledge: London).

Hubler, E. (2004). Helium plant helps Plains Town's economy balloon. The Denver Post. Available at http://www.sandiegouniontribune.com/sdut-helium-plant-helps-plains-towns-economy-balloon-2004jun27-story.html [Verified on 28 November 2017].

Hunt, A. G., Darrah, T. H., and Poreda, R. J. (2012). Determining the source and genetic fingerprint of natural gases using noble gas geochemistry: a northern Appalachian Basin case study. *AAPG Bulletin* **96**(10), 1785–1811. doi:10.1306/03161211093

Jenden, P. D., Newell, K. D., Kaplan, I. R., and Watney, W. L. (1988*a*). Composition and stable-isotope geochemistry of natural gases from Kansas, midcontinent, USA. *Chemical Geology* **71**, 117–147. doi:10.1016/0009-2541(88)90110-6

Jenden, P. D., Kaplan, I. R., Poreda, R. J., and Craig, H. (1988*b*). Origin of nitrogen-rich natural gases in the California Great Valley: evidence from helium, carbon and nitrogen isotope ratios. *Geochimica et Cosmochimica Acta* **52**, 851–861. doi:10.1016/0016-7037(88)90356-0

Jensen, W. (2004). Why helium ends in "ium". *Journal of Chemical Education* **81**, 944. doi:10.1021/ed081p944

Jones, J. K., and Stacey, J. M. (1974). The recovery and liquefaction of helium from natural gas in Poland. *Cryogenics* **14**, 198–202.

Jordan, J. (2016). Helium: a commercial discussion – helium market fundamentals, processing and marketing, IACX Otis Plant case study. In 'AAPG Mid-Continent Section Meeting in Tulsa, Oklahoma, October 4–6 2015'. Search and Discovery Article #70212.

JPDA Production (2017). Available at http://web01.anpm.tl/webs/anptlweb.nsf/vwLafaek/LafaekD67775E50A6FF429CA25770900073AF7 Verified 28 November 2017

Kotarba, M. J., Nagao, K., and Karnkowski, P. H. (2014). Origin of gaseous hydrocarbons, noble gases, carbon dioxide and nitrogen in Carboniferous and Permian strata of the distal part of the Polish Basin: geological and isotopic approach. *Chemical Geology* **383**, 164–179. doi:10.1016/j.chemgeo.2014.06.012

Linde (2010). Inauguration of first helium purification & liquefaction plant of the southern hemisphere at Darwin, Australia. Available at https://linde-kryotechnik.ch/en/inauguration-of-first-helium-purification-liquefaction-plant-of-the-southern-hemisphere-at-darwin-australia [Verified 28 November 2017].

Linde (2017). Global Helium Sources: helium production and capacity 2016–2017. PDF received from Thomas Hagn, Technical Communications, Corporate Communications & IR, The Linde Group, 7 December 2017.

Liu, Y., Zhang, J., Ren, J., Liu, Z., Huang, H., and Tang, X. (2016). Stable isotope geochemistry of the nitrogen-rich gas from lower Cambrian shale in the Yangtze Gorges area, South China. *Marine and Petroleum Geology* **77**, 693–702. doi:10.1016/j.marpetgeo.2016.07.020

Lorant, F., Prinzhofer, A., Behar, F., and Huc, A. Y. (1998). Isotopic (^{13}C) and molecular constraints on the formation and the accumulation of thermogenic hydrocarbon gases. *Chemical Geology* **147**, 249–264. doi:10.1016/S0009-2541(98)00017-5

Main, P. T., Grosjean, E., Edwards, D. S., Boreham, C. J., Chen, J., Hong, Z., and Poreda, R. J. (2014) Distribution and origin of carbon dioxide and helium in natural gas reservoirs of the Browse Basin. In '18th Australian Organic Geochemistry Conference (AOGC) Proceedings: Life, Environments and Resources, 30 November to 2 December 2014, Adelaide' (Eds D. McKirdy and S. Löhr). unpublished.

Manufacturers' Monthly (2010). BOC's helium plant opened in Darwin. Available at http://www.manmonthly.com.au/news/bocs-helium-plant-opened-in-darwin/ [Verified 28 November 2017].

Markiewicz, A., and Winnicki, J. (2013). On geological structure of the Ostrzeszów Hills. *Geological Quarterly* **41**, 347–364. Available at https://gq.pgi.gov.pl/article/view/8238 [Verified 25 March 2018].

McInnes, B., Darrah, T., Hilton, R., Boreham, C., Edwards, D., and Gusterhuber, J. (2017). Investigations into the highest reported He concentration in a natural gas sample: Mt Kitty, Amadeus Basin, Northern Territory. In 'Abstract at Goldschmidt 2017 Conference, Paris, France, August 13–18, 2017'. Available at https://goldschmidt.info/2017/abstracts/abstractView?id=2017003781 [Verified 8 November 2017].

McLaren, S., Sandiford, M., Hand, M., Neumann, N., Wyborn, L., and Bastrakova, I. (2003). The hot southern continent: heat flow and heat production in Australian Proterozoic terranes. *Geological Society of Australia Special Publication* **22**, 151–161.

Merrill, M. D., Löhr, C. D., and Hunt, A. G. (2014). Noble gas geochemistry at the La Barge Platform, Wyoming, USA: CO_2 source and potential total petroleum system investigation tool. In 'American Association of Petroleum Geologists, Rocky Mountain Section, Denver, Colorado, July 20–22 2014'.

Milkov, A. V. (2011). Worldwide distribution and significance of secondary microbial methane formed during petroleum biodegradation in conventional reservoirs. *Organic Geochemistry* **42**, 184–207. doi:10.1016/j.orggeochem.2010.12.003

Moore, M. T., Vinson, D. S., Whyte, C. J., Eymold, W. K., Walsh, T. B., and Darrah, T. H. (2017). Differentiating between biogenic and thermogenic sources of natural gas in coalbed methane reservoirs from the Illinois Basin using noble gas and hydrocarbon geochemistry. In 'Geological Society, London, Special Publications, 468, From Source to Seep: Geochemical Applications in Hydrocarbon Systems' (Eds M. Lawson, M.J. Formolo and J.M. Eiler).

NASA (2001). 'NASA facts - space shuttle use of propellants and fluids'. Vol FS-2001–09–015-KSC. Available at https://www.nasa.gov/centers/kennedy/pdf/167433main_Propellants08.pdf [Verified 8 March 2018].

Nath, B. B. (2013). 'The Story of Helium and the Birth of Astrophysics' (Springer: New York). Available at: https://link.springer.com/book/10.1007%2F978-1-4614-5363-5 [Verified 27 March 2018].

National Materials Advisory Board (2010). 'Selling the Nation's Helium Reserve'. National Research Council (The National Academies Press: Washington, D.C.).

Ni, Y., Dai, J., Tao, S., Wu, X., Liao, F., Wu, W., and Zhang, D. (2014). Helium signatures of gases from the Sichuan Basin, China. *Organic Geochemistry* **74**, 33–43. doi:10.1016/j.orggeochem.2014.03.007

Nuttall, W. J., Cai, Z., Glowacki, B. A., Kazantzis, N., and Clarke, R. H. (2012*a*). The dynamics of the helium market. In 'The Future of Helium as a Natural Resource'. (Eds W.J. Nuttall, R.H. Clarke and B.A. Glowacki) pp. 157–173. (Routledge: London).

Nuttall, W. J., Clarke, R. H., and Glowacki, B. A. (2012*b*). The future of helium. In 'The Future of Helium as a Natural Resource'. (Eds W.J. Nuttall, R.H. Clarke and B.A. Glowacki) pp. 307–312. (Routledge: London).

Octanex (2017). Ascalon retention lease application. Available at http://www.octanex.com.au/publication/view/ascalon-retention-lease-applications/ [Verified 9 March 2018].

Offshore Technology (2016). Bayu-Undan, Timor Sea. Available at http://www.offshore-technology.com/projects/bayu-undan/ [Verified 28 November 2017].

Oil&Gas Journal (2009). ENI starts Blacktip gas field off Australia. Available at http://www.ogj.com/articles/2009/09/eni-starts-blacktip.html [Verified 28 November 2017].

Origin Energy (2016). Annual Reserves Report 29 July 2016. Available at https://www.originenergy.com.au/content/dam/origin/about/investors-media/presentations/160729%20Annual%20Reserves%20Report%202016.pdf [Verified 28 November 2017].

Pacific Oil & Gas (1992). Magee 1, EP38, Northern Territory, Well Completion Report. Available at www.geoscience.nt.gov.au/gemis/ntgsjspui/handle/1/79387 [Verified 8 November 2017]

Peterson, J. B. (2012). The US federal reserve. In 'The Future of Helium as a Natural Resource'. (Eds W.J. Nuttall, R.H. Clarke and B.A. Glowacki) pp. 48–54. (Routledge: London).

Peterson, J. A., and Clarke, J. W. (1983). Petroleum geology and resources of the Volga-Ural Province, U.S.S.R. Geological Survey Circular 885.

Polyak, B. G., and Tolstikhin, I. N. (1985). Isotopic composition of the Earth's helium and the problem of the motive forces of tectogenesis. *Chemical Geology. Isotope Geoscience Section* **52**, 9–33. doi:10.1016/0168-9622(85)90005-3

Poreda, R., and Radicati di Brozolo, F. (1984). Neon isotope variations in Mid-Atlantic Ridge basalts. *Earth and Planetary Science Letters* **69**, 277–289. doi:10.1016/0012-821X(84)90187-0

Poreda, R. J., Jenden, P. D., Kalpan, I. R., and Craig, H. (1986). Mantle helium in Sacramento Basin natural gas wells. *Geochimica et Cosmochimica Acta* **50**, 2847–2853. doi:10.1016/0016-7037(86)90231-0

Poreda, R. J., Craig, H., Arnórsson, S., and Welhan, J. A. (1992). Helium isotopes in Icelandic geothermal systems: I. ^{3}He, gas chemistry, and ^{13}C relations. *Geochimica et Cosmochimica Acta* **56**(12), 4221–4228. doi:10.1016/0016-7037(92)90262-H

Prinzhofer, A. (2013). Noble gas in oil and gas accumulations. In 'The Noble Gases as Geochemical Tracers'. (Ed. P. Burnard) pp. 225–247. (Advances in Isotope Geochemistry, Springer-Verlag: Berlin).

Ramsay, W. (1895). Helium, a gaseous constituent of certain minerals. Part I. *Proceedings of the Royal Society of London* **58**(347–352), 81–89.

Reinoehl, B. (2012). Helium in Algeria - pioneering work for the first large helium plant sourced by tail gases from an LNG facility. In 'The Future of Helium as a Natural Resource'. (Eds W.J. Nuttall, R.H. Clarke and B.A. Glowacki) pp. 55–68. (Routledge: London).

Riley, G. H. (1980). Helium isotopes in energy exploration. *Bulletin of the Australian Society of Exploration Geophysicists* **11**, 14–18. doi:10.1071/EG980014

Rufford, T. E., Chan, K. I., Huang, S. H., and May, E. F. (2014). A review of conventional and emerging process technologies for the recovery of helium from natural gas. *Adsorption Science and Technology* **32**, 49–72. doi:10.1260/0263-6174.32.1.49

Sano, Y., Marty, B., and Burnard, P. (2013). Noble gases in the atmosphere. In 'The Noble Gases as Geochemical Tracers'. (Ed. P. Burnard) pp. 17–31. (Advances in Isotope Geochemistry, Springer-Verlag: Berlin).

Santos (2017). 2017 Investor Day Presentation. Available at https://www.santos.com/media-centre/announcements/2017-investor-day-presentation/ Slide 62 in pdf [Verified 23 January 2018].

Sarda, P., Staudacher, T., and Allègre, C. J. (1988). Neon isotopes in submarine basalts. *Earth and Planetary Science Letters* **91**, 73–88. doi:10.1016/0012-821X(88)90152-5

Sathaye, K. J., Larson, T. E., and Hesse, M. A. (2016). Noble gas fractionation during subsurface gas migration. *Earth and Planetary Science Letters* **450**, 1–9. doi:10.1016/j.epsl.2016.05.034

Scurlock, R., and Francis, A. (2012). Is there a helium problem? In 'The Future of Helium as a Natural Resource'. (Eds W.J. Nuttall, R.H. Clarke and B.A. Glowacki) pp. 296–306. (Routledge: London).

Seibel, C. W., and Kennedy, H. S. (1934). Helium. In 'USGS Minerals Yearbook, 1934'. pp 867–870.

Shelton, J. L., McIntosh, J. C., Hunt, A. G., Beebe, T. L., Parker, A. D., Warwick, P. D., Drake Ii, R. M., and McCray, J. E. (2016). Determining CO_2 storage potential during miscible CO_2 enhanced oil recovery: noble gas and stable isotope tracers. *International Journal of Greenhouse Gas Control* **51**, 239–253. doi:10.1016/j.ijggc.2016.05.008

Skirrow, R. G., Huston, D. L., Mernagh, T. P., Thorne, J. P., Dulfer, H., and Senior, A. B. (2013). Critical commodities for a high-tech world: Australia's potential to supply global demand. Geoscience Australia, Canberra. Available at https://ecat.ga.gov.au/geonetwork/srv/eng/search#!dfdb8e16-3c25-0990-e044-00144fdd4fa6 [Verified 28 November 2017].

Smith, D. M., Goodwin, T. W., and Schillinger, J. A. (2004). Challenges to the worldwide supply of helium in the next decade. *American Institute of Physics Conference Proceedings* **710**, 119–138.

Snyder, G., Poreda, R., Hunt, A. G., and Fehn, U. (2001). Regional variations in volatile composition: isotopic evidence for carbonate recycling in the Central American volcanic arc. *Geochemistry Geophysics Geosystems* **2**, 1057. doi:10.1029/2001GC000163

Tade, M. D. (1967). Helium storage in Cliffside Field. *Journal of Petroleum Technology* **19**, 885–888. doi:10.2118/1624-PA

Tao, S., Zou, C., Mi, J., Gao, X., Yang, C., Zhang, X., and Fan, J. (2014). Geochemical comparison between gas in fluid inclusions and gas produced from the Upper Triassic Xujiahe Formation, Sichuan Basin, and SW China. *Organic Geochemistry* **74**, 59–65. doi:10.1016/j.orggeochem.2014.05.008

Tenthorey, E., Boreham, C. J., Hortle, A. L., Underschultz, J. R., and Golding, S. D. (2011). Importance of mineral sequestration during CO_2 gas migration: a case study from the Greater Gorgon area. *Energy Procedia* **4**, 5074–5078. doi:10.1016/j.egypro.2011.02.481

Tolstikhin, I. N., and Marty, B. (1998). The evolution of terrestrial volatiles: a view from helium, neon, argon and nitrogen isotope modelling. *Chemical Geology* **147**, 27–52. doi:10.1016/S0009-2541(97)00170-8

Tongish, C. A. (1980). Helium - its relationship to geologic systems and its occurrence with the natural gases, nitrogen, carbon dioxide, and argon. United States Department of the Interior Report of Investigation 8444, 176pp.

USGS (US Geological Survey) (2007). Mineral Commodity Summaries, January 2007, pp. 76–77. Available at https://minerals.usgs.gov/minerals/pubs/commodity/helium/heliumcs07.pdf [Verified 8 November 2017].

USGS (US Geological Survey) (2012). Mineral Commodity Summaries, January 2013, pp. 72–73. Available at https://minerals.usgs.gov/minerals/pubs/commodity/helium/mcs-2013-heliu.pdf [Verified 8 November 2017].

USGS (US Geological Survey) (2017*a*). Mineral Commodity Summaries 2017: US Geological Survey, 202pp. Available at https://doi.org/10.3133/70180197 [Verified 8 November 2017].

USGS (US Geological Survey) (2017*b*). Mineral Commodity Summaries, January 2017, pp. 78–79. Available at https://minerals.usgs.gov/minerals/pubs/commodity/helium/mcs-2017-heliu.pdf [Verified 8 November 2017].

Ward, D. E., and Pierce, A. P. (1973). Helium. In 'United States Mineral Resources. Geological Survey Professional Paper 820'. (Eds D.A. Brobst and W.P. Pratt) pp. 285–290.

Watson, M. N., Boreham, C. J., and Tingate, P. R. (2004). Carbon dioxide and carbonate cements in the Otway Basin: implications for geological storage of carbon dioxide. *The APPEA Journal* **44**(1), 703–720. doi:10.1071/AJ03035

Woodside (2016*a*). Annual Report 2015: Strength through resilience. Available at http://www.woodside.com.au/Investors-Media/announcements/Documents/17.02.2016%202015%20Annual%20Report.PDF [Verified 28 November 2017].

Woodside (2016*b*). ASX Announcement 5 September 2016. Available at http://www.woodside.com.au/Investors-Media/announcements/Documents/Woodside%20agrees%20to%20acquire%20half%20of%20BHPBs%20Scarborough%20assets.pdf [Verified 28 November 2017].

Xu, Y., Shen, P., Sun, M., and Xu, S. (1991). Non-hydrocarbon and noble gas geochemistry. *Journal of Southeast Asian Earth Sciences* **5**, 327–332. doi:10.1016/0743-9547(91)90044-X

Yurkowski, M. M. (2016). Helium in Southwestern Saskatchewan: Accumulation and Geological Setting. Open File Report 2016–1. Government of Saskatchewan.

Zartman, R. E., Wasserburg, G. J., and Reynolds, J. H. (1961). Helium, argon, and carbon in some natural gases. *Journal of Geophysical Research* **66**, 277–306. doi:10.1029/JZ066i001p00277

The authors

Chris Boreham obtained his PhD in Chemistry at the Australian Nation University and has worked at GA for over three decades. He is an internationally recognised petroleum geochemist with experience ranging from the application of organic geochemistry to the evolution of oil and gas in sedimentary basins. More recently he has extended these geochemical studies to unconventional petroleum (coal seam methane, shale gas and oil). He also leads key aspects of the CO2CRC's studies on the injection of CO_2 into a depleted natural gas field and a saline aquifer.

Dianne Edwards is a senior petroleum geochemist in GA's Resources Division, Energy Systems Branch. Her scientific focus is on defining the petroleum systems of Australia's petroliferous basins including both conventional and unconventional play types. Dianne received her BSc (Hons) degree in Geology and MSc in Organic Petrology and Organic Geochemistry from the University of Newcastle-upon-Tyne (UK). She was awarded her PhD from the University of Adelaide in 1996. Dianne is a member of PESA.

Robert Poreda received his PhD from the University of San Diego in 1983 and is a professor in the Department of Earth and Environmental Sciences at the University of Rochester (Rochester, New York). He completed his PhD from Scripps Institute of Oceanography in 1983. His current research interests include applying noble gas and gas isotope geochemistry to research on fluid migration within the crust of the Earth, water masses and atmosphere.

Tom Darrah obtained his PhD in Geochemistry at the University of Rochester, Rochester, New York, USA. He currently works as an Associate Professor at The Ohio State University, the Director of the Ohio State University Noble Gas Laboratory and Co-Director of the Ohio State University Subsurface Energy Research Center. He is an internationally recognised petroleum geochemist with experience in the application of noble gas and stable isotopes geochemistry to fluid transport in sedimentary basins. He has recently developed noble gas applications to understand unconventional petroleum systems (shale gas, coalbed methane, helium resources, CO_2 resources), the environmental impacts of unconventional energy development (stray gas migration), and enhanced oil recovery.

Ron (Zhong Rong) Zhu (BSc, MSc, PhD), is a petroleum geologist with the Resources Division of GA. After he received his PhD from the Australian National University in 1990, he worked in the School of Applied Geology and Western Australian School of Mines at Curtin University, as well as in several private resources companies in Perth. Dr Zhu joined GA in 2002. His present work focuses on managing Australia's petroleum resource information and providing technical advice to the Federal Government on petroleum resource issues.

Emmanuelle Grosjean received her PhD in organic geochemistry from the University of Strasbourg (France) in 2002 and subsequently spent three post-doctoral years at the Massachusetts Institute of Technology working on the Precambrian petroleum systems of the South Oman Salt Basin. Emmanuelle joined GA in 2005 to work on the detection of natural hydrocarbon seepage in Australia. She has since been involved in several studies focussed on the petroleum prospectivity of Australia's sedimentary basins.

Philip Main is a geochemist and has been working in the Mineral System Branch at GA since 2014. He currently is working on surface geochemistry of regional areas using low-density sampling. Philip has a BSc (Hons) from the University of Queensland.

Kathryn Waltenberg is a geochronologist and isotope geoscientist at GA. Kathryn has a PhD in geochronology from the University of Queensland and is a member of the Geological Society of Australia.

Paul A. Henson graduated from the University of Tasmania and is currently managing the Onshore Energy Systems Section at GA. He has extensive experience in the minerals sector working on mineral systems in Proterozoic and Archaean terranes. Since 2010 he has led the Australian Governments' onshore carbon storage program, undertaking deep onshore drilling and seismic acquisition programs in collaboration with the states and industry. In addition, he now manages the Exploring for the Future - Energy Program, leading a team of researchers to acquire new pre-competitive geoscientific data to improve our understanding of the hydrocarbon potential of Australian onshore basins.